



**Transverse Emittance Measurement with the Three-Monitor-Method at the CERN Linac4**

K. Hanke, T. Hermanns, B. Mikulec

**Abstract**

This report evaluates the applicability of the Three-Monitor-Method to determine the transverse emittance of the CERN Linac4 160 MeV H<sup>-</sup>-beam. The Three-Monitor-Method is a linear formalism allowing to calculate transverse emittance values from beam size measurements at three different positions along a beam line, assuming that the transfer matrix elements between these locations are known. It is planned to build two of these measurement systems, which should operate from 2013/14 immediately behind the exit of the linear accelerator in the dump line and close to the end of the transfer line to the PS Booster synchrotron in the LBE line.

At first, the mathematical formalism and the simulation tools are briefly introduced. Then, the method is applied for both measurement lines. Results on measurement precisions and systematic errors are presented. Final conclusions are drawn at the end, and a summary of the equipment to be installed or modified will be given.

BE-OP  
Ref. Linac4

# Transverse Emittance Measurement with the Three-Monitor-Method at the CERN Linac4

K. Hanke, T. Hermanns, B. Mikulec  
CERN, 1211 Geneva 23, Switzerland

Geneva, November 23, 2009

## Abstract

This report evaluates the applicability of the Three-Monitor-Method to determine the transverse emittance of the CERN Linac4 160 MeV H<sup>-</sup>-beam. The Three-Monitor-Method is a linear formalism allowing to calculate transverse emittance values from beam size measurements at three different positions along a beam line, assuming that the transfer matrix elements between these locations are known. It is planned to build two of these measurement systems, which should operate from 2013/14 immediately behind the exit of the linear accelerator in the *dump line* and close to the end of the transfer line to the PS Booster synchrotron in the *LBE line*.

At first, the mathematical formalism and the simulation tools are briefly introduced. Then, the method is applied for both measurement lines. Results on measurement precisions and systematic errors are presented. Final conclusions are drawn at the end, and a summary of the equipment to be installed or modified will be given.

Contact corresponding authors: [Thomas.Hermanns@cern.ch](mailto:Thomas.Hermanns@cern.ch) and [Bettina.Mikulec@cern.ch](mailto:Bettina.Mikulec@cern.ch)

# Table of Contents

<b>Abstract</b>	<b>1</b>
<b>1 Introduction</b>	<b>1</b>
1.1 Mathematical Formalism . . . . .	1
1.2 Limitations and Assumptions of the Method . . . . .	2
1.3 Simulation Tools and Method . . . . .	3
1.4 Monitor Type for Beam Size Measurement Procedure . . . . .	4
<b>2 Linac4 Dump Line</b>	<b>4</b>
2.1 Linac4 Dump Line Simulations . . . . .	4
2.2 Reconstruction of the Transverse Emittances . . . . .	6
2.3 Simulation Results for the Nominal Beam . . . . .	9
2.4 Varying Linac4 Beam Current . . . . .	9
2.5 Varying Longitudinal Input Parameters . . . . .	11
2.6 Limitations . . . . .	11
<b>3 LBE Line</b>	<b>12</b>
3.1 LBE Line Simulations . . . . .	12
3.2 Reconstruction of Transverse Emittance Values and Phase Space Ellipses . . . . .	14
3.3 Simulation Results for the Nominal Beam . . . . .	15
3.4 Systematic Studies . . . . .	17
3.5 Measurement with more than Three Monitors . . . . .	19
<b>4 Summary and Conclusions</b>	<b>21</b>
<b>A Configuration File for the Linac4 Dump Line in TRACE 3-D</b>	<b>23</b>
<b>B Configuration File for the LBE Line in TRACE 3-D</b>	<b>23</b>
<b>C Further Results for the LBE Line</b>	<b>25</b>
<b>List of Figures</b>	<b>26</b>
<b>List of Tables</b>	<b>26</b>
<b>References</b>	<b>27</b>

# 1 Introduction

The transverse emittance of the Linac4 160 MeV H<sup>-</sup>-beam is intended to be measured at two different locations behind the exit of the accelerator. For commissioning of Linac4 and as permanent operational check it is required to stay as close as possible to the Linac4 exit. Therefore, it is proposed to install a measurement system in the Linac4 dump line. For commissioning of the transfer line between Linac4 and PS Booster and for operational surveillance of the transverse emittance before injecting the beam into the PS Booster the already existing LBE line is considered to be upgraded. It is simulated if the method of an emittance determination using beam size measurements with three (and more) beam monitors leads to satisfying results at both locations.

In the following introductory chapter this report briefly summarizes the method and presents the simulation tools which have been used for the studies. Subsequently, chapter 2 and chapter 3 deal with the measurement aspects for the dump line and the LBE line. After a layout description the individual input parameters as well as results of simulations and systematic error studies are given. In chapter 4 conclusions are drawn addressing the main question if and how the method can be used to determine the transverse emittance of the Linac4 beam behind the linear accelerator. Chp. 2  
Chp. 3  
Chp. 4

## 1.1 Mathematical Formalism

The beam as an ensemble of particles is described in two-dimensional phase space with the phase space vector  $\vec{v} = (x, x')^T$  (space coordinate  $x$  and momentum/angle coordinate  $x'$ ) by an ellipse enclosing the particles<sup>1</sup>

$$\gamma x^2 + 2\alpha x x' + \beta x'^2 = \varepsilon \quad (1)$$

In this notation the Twiss parameters  $\alpha$ ,  $\beta$ , and  $\gamma$  determine the shape and orientation of the ellipse, while the area covered by the ellipse is represented by  $\pi\varepsilon$  with *beam emittance*  $\varepsilon$ . If the beam is propagating along a beam line, the shape and orientation of the ellipse can change, but the area of the ellipse remains constant (Liouville's theorem). The evolution of the entire beam can be described by the evolution of this boundary ellipse, because even if a single particle of the whole ensemble is parametrized by its own ellipse, the particle trajectories lie and more importantly remain either inside or on this boundary ellipse.

Therefore, in a two-dimensional matrix representation the beam is described by the *beam sigma matrix*

$$\Sigma = \varepsilon \cdot \begin{bmatrix} \beta & -\alpha \\ -\alpha & \gamma \end{bmatrix}, \quad (2)$$

with  $\det(\Sigma) = \varepsilon^2$ , and the dedicated ellipse at any point in phase space reads like follows

$$\vec{v}^T \Sigma^{-1} \vec{v} = 1. \quad (3)$$

The general propagation in phase space between a reference point  $\vec{v}_0$  and any point of a beam line  $\vec{v}$  is realized by means of a transfer matrix  $R$

$$\vec{v} = R \vec{v}_0 \quad \text{with } R = \begin{bmatrix} C & S \\ C' & S' \end{bmatrix}, \quad (4)$$

which contains the cosine- and sine-like solutions  $C$  and  $S$  and their derivatives for the betatron motion between these two points. If this transfer equation is inserted into equation 3 defined for a reference point (index 0) in the beam line, the following relation is obtained.

$$\begin{aligned} \vec{v}_0^T \Sigma_0^{-1} \vec{v}_0 &= (R^{-1} \vec{v})^T \Sigma_0^{-1} (R^{-1} \vec{v}) \\ &= \vec{v}^T \cdot (R^{-1})^T \Sigma_0^{-1} \cdot (R^{-1}) \vec{v} \\ &= \vec{v}^T \cdot \underbrace{[R \Sigma_0 R^T]^{-1}}_{\Sigma^{-1}} \cdot \vec{v} \end{aligned} \quad (5)$$

$$\Rightarrow \Sigma = R \Sigma_0 R^T$$

<sup>1</sup>In this report all phase space considerations are valid for the horizontal and vertical plane unless explicitly distinguished. In this sense the phase space vector  $\vec{v} = (x, x')^T$  stands for both transverse planes.

This equation reveals that the evolution of phase space coordinates can be transferred to the evolution of the ellipse parameters, which reads in a three-dimensional representation as follows.

$$\begin{pmatrix} \beta \\ \alpha \\ \gamma \end{pmatrix} = \begin{bmatrix} C^2 & -2CS & S^2 \\ -CC' & CS' + SC' & -SS' \\ C'^2 & -2C'S' & S'^2 \end{bmatrix} \begin{pmatrix} \beta_0 \\ \alpha_0 \\ \gamma_0 \end{pmatrix} \quad (6)$$

Furthermore, there is a proportionality between squared beam size  $\sigma^2$  and parameter  $\beta$  by means of the emittance

$$\sigma^2 = \varepsilon \cdot \beta. \quad (7)$$

Inserting this equation into the evolution equation 6 for  $\beta$  (only first line), the parameters  $\alpha_0$ ,  $\beta_0$  and  $\varepsilon$  at the reference point can be calculated if the beam size for at least three locations along the beam line is measured. This requires that the transfer matrices between the reference point and each measurement point are known from the optical design of the beam line. Three measurements are sufficient because from geometrical considerations it can be deduced that the three ellipse parameters fulfill  $\gamma\beta - \alpha^2 = 1$  such that in general  $\gamma$  is replaced by  $\alpha$  and  $\beta$ . Thus, only the emittance and two out of the three beam parameters are independent values.

Hence, in solving the linear equation system

$$M \cdot \vec{b} - \vec{\sigma}^2 = 0 \quad \text{with } M = \begin{bmatrix} C_1^2 & -2C_1S_1 & S_1^2 \\ C_2^2 & -2C_2S_2 & S_2^2 \\ C_3^2 & -2C_3S_3 & S_3^2 \end{bmatrix} \quad (8)$$

for  $\vec{b} = (\varepsilon\beta_0, \varepsilon\alpha_0, \varepsilon\gamma_0)^T$ , one obtains the desired result.

Technically, the emittance measurement is split into a measurement of beam sizes, while the transfer matrix elements must be provided by a simulation code, which takes the geometrical and optical design of the beam line as input. Further details and explanations on this approach are given in [1].

Ref. [1]

The matrix  $M$  is not restricted to be a  $3 \times 3$ -matrix, but can become a  $N \times 3$ -matrix if  $N > 3$  beam size measurement systems are installed. In that case the equation system is overdetermined and the solution for the three-dimensional vector  $\vec{b}$  cannot be determined analytically anymore, but must be assessed numerically, for instance by least-square approximations. On the other hand more measurements allow for calculating further beam parameters like dispersion and relative momentum spread, so that the dimension of  $\vec{b}$  is increased.

## 1.2 Limitations and Assumptions of the Method

As the matrix  $M$  is composed of linear transfer matrix elements to the measurement positions, emittance values are calculated only in linear approximations, too. Thus, it is questionable if meaningful results can still be obtained when non-linear contributions due to space charge effects are neglected or only approximatively modeled. But there are a few more assumptions of the method listed here.

- The transfer matrices between the monitors have to be known with sufficient precision.
- The emittance should be approximately constant along the measurement section such that each monitor probes the same emittance value.
- The phase space planes must be decoupled throughout the entire measurement section.
- In order to get true values for  $\vec{b}$ , the beam sizes must be corrected for dispersion effects, as the total, i.e. measured, beam size  $\sigma$  is the sum of two contributions

$$\sigma_{total} = \sqrt{\sigma_{true}^2 + \left(D \frac{dp}{p}\right)^2} \quad (9)$$

with dispersion function  $D$  and relative momentum spread  $\frac{dp}{p}$ . Thus, the best solution is to perform the measurement in a dispersion-free area, or if not possible to derive  $D$  and  $\frac{dp}{p}$  from simulations or from additional beam-size measurements.

- For three measurements the phase space ellipse is theoretically best sampled if it rotates in phase space by about  $60^\circ$  between successive positions. This implies in the here-studied lines that the measurement at the mid-position is done close to a beam waist, the minimum of the beta-function, which imposes an inevitable constraint on the design of the measurement lines.

### 1.3 Simulation Tools and Method

For the simulation studies two programs are used: TRACE 3-D [2] and Path [3]. From these two programs, transfer matrices (TRACE 3-D), beam sizes (Path) and reference ellipse parameters (Path) are obtained. For all simulations H<sup>-</sup> ions with mass  $m = 939.294 \text{ MeV}$  and charge  $q = -1e$  are assumed. Furthermore, to account for electromagnetic interactions between the charged particles, the maximum expected beam current of 65 mA is set in most cases. Ref. [2]  
Ref. [3]

The design of both lines is done with the TRACE 3-D code. This program models a beam as an uniformly filled ellipsoid propagating a  $5\sigma$ -beam envelope through the beam line with all phase space planes being decoupled. At first, the geometrical and optical layout of the line is implemented and optimal positions of the beam monitors are identified. Then, the code is used to obtain the *transfer matrices between the beam monitors*, which respects electromagnetic interactions due to the non-zero input value for the beam current, assuming a homogeneous charge density within the ellipsoid. Hence, the transfer matrices are not only given in pure linear approximation, but space charge effects are respected to a certain extent as well. Finally, values for dispersion and relative momentum spread to correct the beam sizes can be extracted from TRACE 3-D. The numerical precision of the code is limited to  $10^{-6}$ , which is sufficiently high for the present studies.

Path is used to provide the *beam sizes at the three monitor positions* and the *reference value for the emittance* to which the calculated emittance is compared. The Path code tracks single particles through the beam line. The output of Path simulations of the Linac4 line (for the dump line) and the transfer line to the PS Booster (for the LBE line) have been taken as input distributions to the present studies for the dump line and LBE line, respectively. Both data-sets correspond to a sample of about 42000 H<sup>-</sup> ions. In order to reduce the computing time, the beam is separated into uniformly charged rings to approximate the space charge effects instead of considering particle-by-particle interactions. It is not possible to derive the transfer matrices by Path because they are calculated only from a single particles, therefore not allowing to include space charge effects. The beam line layout defined with the TRACE 3-D program is implemented and at the selected positions of the beam size monitors the RMS beam sizes are determined. Once Linac4 will be operating, transfer matrices will be taken from the TRACE 3-D simulations, but the Path output will be replaced by real measurements.

For systematic studies both programs are used according to their task in the simulation procedure. Errors in the matrix elements are assessed by TRACE 3-D, while alignment errors of the beam line components as well as errors in the optical design and their effects on the beam size measurements are covered by Path.

The measurement and a finite resolution of the beam monitors is simulated by statistical tools as well. At the monitor positions histograms are filled with the horizontal and vertical coordinates of all particles. Thereby, the bin width of the histograms is adapted to one of six potential resolution values (10  $\mu\text{m}$ , 50  $\mu\text{m}$ , 100  $\mu\text{m}$ , 200  $\mu\text{m}$ , 500  $\mu\text{m}$ , and 1000  $\mu\text{m}$ ). Then, each distribution is fitted by a Gaussian function using a binned maximum likelihood algorithm to determine the best solution [4]. The width of the Gaussian function serves as beam size, with an uncertainty given by the fit parameter error. Ref. [4]

The output of TRACE 3-D, Path and from the beam size fits serves as input to a Mathematica script, in which the mathematical formalism of chapter 1.1 is implemented. The calculated emittance is then compared to the emittance value at the position of the first monitor simulated with Path, but any other position could be used as well. Chp. 1.1

In order to numerically assess the quality of the reconstructed values the relative difference of each parameter to its reference value is calculated. In addition, a more global geometric mismatch coefficient  $\Delta J$  can be defined as well. This is the determinant of the difference matrix, which one gets if the reconstructed beam matrix  $\Sigma_{reco}$  is subtracted from the reference matrix  $\Sigma_0$ <sup>2</sup> (see equation 2).

$$\Delta J = \det \begin{bmatrix} \beta_0 - \beta_{reco} & -(\alpha_0 - \alpha_{reco}) \\ -(\alpha_0 - \alpha_{reco}) & \gamma - \gamma_{reco} \end{bmatrix}, \quad (10)$$

<sup>2</sup>For this special consideration of the deviation of  $\alpha$  and  $\beta$  the emittance is assumed to be constant and therefore neglected as an overall scaling factor.

Fig. 1 A schematic drawing illustrates the use of the simulation packages for the present study (see Figure 1).

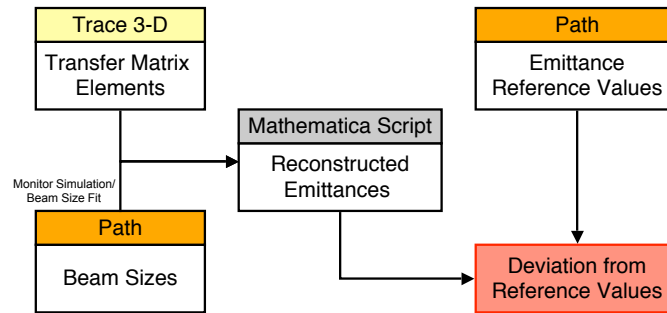


Figure 1: Analysis flow of the emittance measurement with the Three-Monitor-Method.

## 1.4 Monitor Type for Beam Size Measurement Procedure

For a beam size measurement the interactions of the H<sup>-</sup> ions with the detector material cannot be neglected. If the H<sup>-</sup> beam passes through a real monitor, the electrons will be stripped off after only a few tenths of micrometers. Thus, it must be examined if the two stripped electrons do not artificially enlarge the beam size and spoil the measurement resolution. In addition, the energy deposited in the detector must not heat up the material or deteriorate it otherwise. These two aspects are addressed in a note [5] where it is proposed to use 1 mm thick alumina screens read out with appropriate cameras<sup>3</sup>. The most important operational consequence is that the pulse length must be restricted to 100 μs to keep the instantaneous temperature increase due to the beam impact to an acceptable limit. This is actually not an additional limitation, as the beam dumps both in the dump line and the LBE line are anyway designed for a maximum beam pulse length of 100 μs. An interlock will assure this condition and protect monitors and dumps.

Concerning the measurement procedure it must be taken into account that the phase space distributions of the particles changes when they interact with the detector material [6]. This influences the measured beam sizes at the second and third monitor as multiple scattering would blow up the beam size to a non acceptable extent. Thus, the proposed solution is to measure the beam sizes at each monitor not with the same bunch of particles, but with successive ones. This procedure would increase the measurement time and be sensitive to pulse-to-pulse variations, but it would still be faster and less complicated than a quadrupole scan.

In principle it would also be possible to measure the beam sizes with the same bunch and apply correction functions on the measured values of the second and third monitor. This procedure would still have to be investigated, but it is clear that these corrections would depend on the chosen model for the simulation of the interactions and therefore would be affected by an intrinsic systematic error.

## 2 Linac4 Dump Line

Linac4 will be commissioned in the year 2013. During this period it is essential to measure the transverse emittance of the beam at the end of the linac to optimise different machine parameters. Later on, the emittance measurement will be needed in addition if emittance-blow up would be observed downstream or if parameters would change in the linac. As there will be a dump installed after the Linac4 exit, it has been decided to perform the transverse emittance measurements in this Linac4 dump line.

### 2.1 Linac4 Dump Line Simulations

The Linac4 dump line starts after the horizontal bending magnet that sends the beam down a new transfer line, which will then join the second part of the currently used Linac2 transfer line going to the PS Booster. Beam distributions for the Linac4 peak current (65 mA) at the exit of Linac4 have been provided by the Linac4 beam

<sup>3</sup>The cameras will be optimised to achieve the desired resolution. Optimum positions and shielding for the cameras still have to be studied to minimise radiation damage mainly due to dump back-scattering.

dynamics working group and used as input for the emittance simulations (see Figure 2 showing the phase space Fig. 2 distributions of the beam at the Linac4 exit). Therefore, the start of the new transfer line between the last accelerating structure (pi-mode structure, PIMS) until the first horizontal bending magnet has been included in the TRACE 3-D model of the line.

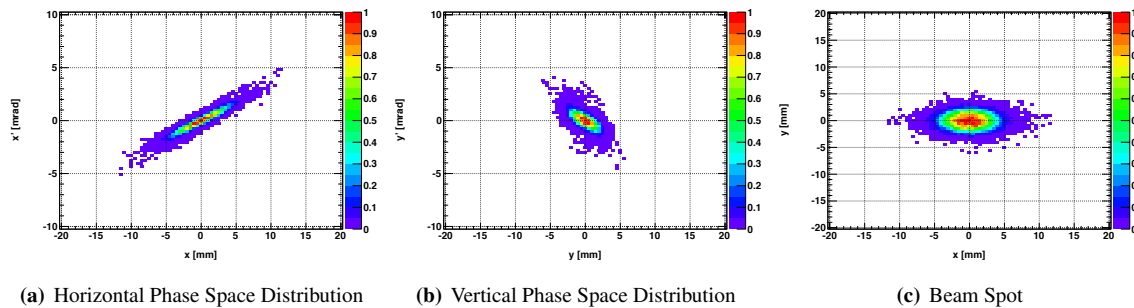


**Figure 2:** Phase space distributions and two-dimensional beam size of the H-beam as coming out of Linac4.

A schematic drawing of the layout of the line between the Linac4 exit and the Linac4 dump is shown in Figure 3. Fig. 3 The total length of this line (until the end of the dump) is 13.9 m, with the front face of the bending magnet located at 3.14 m, and the beginning of the Linac4 dump (concrete shielding) at 10.3 m distance from the Linac4 exit. The two steerers will allow to center the beam on the monitors and the dump. There will almost certainly be some minor modifications to this layout; some beam instrumentation equipment might be moved or added, and the position of the dump has not yet been finalised. Upstream, the PIMS will also undergo small changes that will slightly affect the input beam distribution.

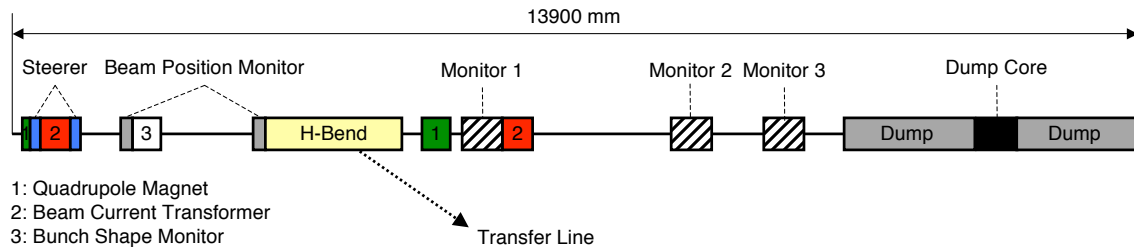


**Figure 3:** Schematic layout of the Linac4 dump line. Between the Linac4 exit and the bending magnet the following elements will be installed: a quadrupole magnet, a beam current transformer, a horizontal and a vertical steerer magnet with two beam position monitors and a bunch shape monitor. The horizontal bending magnet (H-Bend) allows to send the beam either to the Linac4 dump (magnetic field set to zero) or to the new transfer line direction PS Booster (bending angle:  $35^\circ$ ). For the Three-Monitor emittance measurement a second quadrupole will be added after the horizontal bending as well as three monitors. Another beam transformer will allow to measure the percentage of beam being sent to the dump.

The layout of Figure 3 has been implemented in TRACE 3-D (refer to appendix A for the configuration file). The Fig. 3 position of the three monitors has been chosen such that for both horizontal and vertical transverse emittance measurements and using the same monitor positions the phase space ellipses turn by approximately  $60^\circ$  between the monitors for optimum sampling of the ellipses. The two quadrupoles are used to produce a beam waist close to the central monitor for this purpose. There are two different sets of field gradients, one for the horizontal and one for the vertical emittance measurement<sup>4</sup>. These quadrupole field gradients and the input beam parameters can be found in Table 1. Tab. 1

Table 2 gives an overview on the location of the three monitors (distance in mm counted from the Linac4 exit), Tab. 2 the beam ellipse parameters and the simulated RMS beam sizes and emittances at the three monitor locations. Monitor 2 is at 2.60 m distance from monitor 1, monitor 3 is 3.76 m downstream of monitor 1. The differences in angle of the phase space ellipses between the three monitor positions can then be deduced. They are very

<sup>4</sup>As the two quadrupoles will be of a different design, the limit of the field gradient for the first one (Linac4 accelerator type) is around 20 T/m and for the second quadrupole (transfer line type) around 11.4 T/m.



	$\alpha$	$\beta$	$\varepsilon(1\sigma)$
horizontal	-3.397	10.024 mm/mrad	0.570 mm mrad
vertical	0.971	2.714 mm/mrad	0.542 mm mrad
longitudinal	-0.131	0.028 deg/keV	177.749 deg keV
	Quad 1	Quad 2	
horizontal plane	1.0 T/m	-2.5 T/m	
vertical plane	-13.0 T/m	2.8 T/m	

**Table 1:** Input parameters of the 65 mA Linac4 H-beam for the TRACE 3-D Linac4 dump line simulations. Settings of the quadrupole magnets for the emittance measurements in the horizontal and vertical plane are also given.

close to the theoretically best value of  $60^\circ$ .

$$\begin{aligned} \Delta\varphi_{12}^{\text{hor}} &= 53.64^\circ & \Delta\varphi_{12}^{\text{ver}} &= 54.11^\circ \\ \Delta\varphi_{23}^{\text{hor}} &= 57.80^\circ & \Delta\varphi_{23}^{\text{ver}} &= 58.98^\circ \end{aligned} \quad (11)$$

	Monitor Position [mm]	$\alpha$	$\beta$ [mm/mrad]	$\varphi$	$r(1\sigma)$ [mm]	$\varepsilon(1\sigma)$ [mm mrad]
horizontal plane	5790	28.777	82.896	160.85°	6.9	0.5698
	8390	2.952	1.009	107.21°	0.8	0.5698
	9550	-8.250	7.128	49.41°	2.0	0.5698
vertical plane	5790	11.480	32.422	160.49°	4.2	0.5422
	8390	1.025	0.549	106.38°	0.5	0.5422
	9550	-3.345	3.222	47.40°	1.3	0.5422

**Table 2:** Positions of the beam monitors (distance from Linac4 exit), ellipse parameters and expected beam sizes at the three beam monitor positions as determined by TRACE 3-D for 65 mA beam current. With TRACE 3-D the (unnormalised) emittances stay constant.

It is possible to obtain from the TRACE 3-D code transfer matrices that include space charge effects under the approximation of a uniformly filled beam ellipse. For convenience<sup>5</sup>, the reference point is chosen to be at the position of monitor 1. The resulting cosine- and sine-like elements of the transfer matrices relevant for the measurements in the horizontal and vertical plane, respectively, are given in Table 3. The indices refer to the monitor position, for which the transfer matrix has been calculated with respect to the reference point (monitor 1).

Tab. 3

	$C_1$	$S_1$	$C_2$	$S_2$	$C_3$	$S_3$
horizontal plane	1.0	0.0	1.013855	2.616053	1.063153	3.896250
vertical plane	1.0	0.0	1.036168	2.639604	1.116243	3.972720

**Table 3:** Cosine- and sine-like elements of the transfer matrices between the reference point at the first monitor position and the three monitor positions.

## 2.2 Reconstruction of the Transverse Emittances

Besides the relevant elements of the transfer matrices  $C_i$  and  $S_i$ , it is required to know the RMS beam sizes at the three monitor positions to calculate the emittance with equation 8. For this purpose the simulation program Path has been used. It also serves to provide the reference values for the transverse emittance and the beam parameters to cross-check the deviations of the calculated values. The reference phase space distributions at the position of monitor 1 can be seen in Figure 4.

Fig. 4

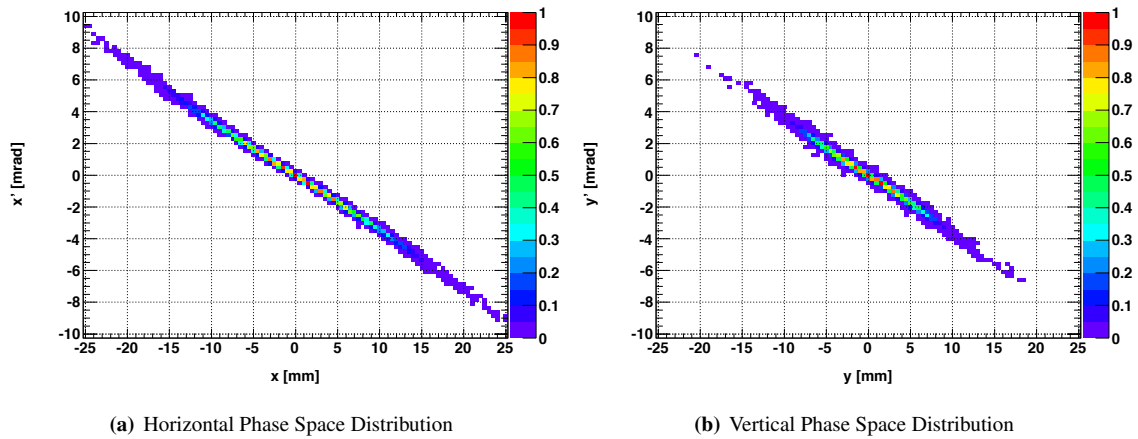


**Figure 4:** Reference phase space distributions at the location of monitor 1 in horizontal (left) and vertical (right) plane for the quadrupole settings during horizontal emittance measurement (left) and vertical measurement (right) and 65 mA beam current.

Furthermore, the transverse emittance evolution and the evolution of RMS beam sizes for a horizontal or vertical emittance measurement are illustrated in Figure 5 and Figure 6. It can be seen that the emittance evolution as calculated by Path with the quadrupole configuration for the horizontal or the vertical emittance measurement stays approximately constant in the region of the three monitors (the emittance growth between the first and the third monitor amounts to 6.0%/3.7% for the horizontal/vertical case, respectively). For the Path simulations, a uniform small step size of 2 cm has been implemented along the line. The beam sizes at the three monitors for the horizontal and vertical emittance measurement are summarised in Table 4.

Fig. 5  
Fig. 6

Tab. 4

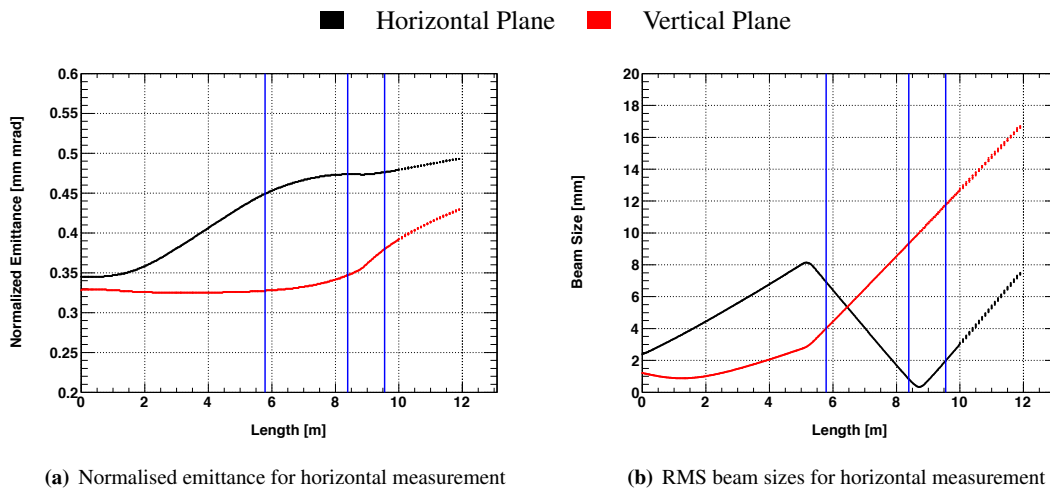


**Figure 5:** Emittance and RMS beam size evolution along the line as simulated with Path for the horizontal emittance measurement. The vertical blue lines indicate the three monitor positions.

As it will not be possible to determine the beam sizes with nm measurement precision, adequate monitor resolutions must be selected. In Figure 7 the evolution of the deviation of the reconstructed emittances from their reference values at monitor 1 versus different monitor resolutions are depicted. The resolution values given in this plot have been assumed to be common for all three monitors. The error band is given by the maximum and minimum deviation if the fitted beam sizes are varied by plus and minus their fitting parameter error (8 possible combinations). For each of the six measurement precisions, the error leading to the largest deviation has been chosen; therefore the resulting error corresponds to the worst possible case, but it is still below 10%, the target value for the maximum tolerable error in the determination of the emittance.

Fig. 7

<sup>5</sup>In this case the first transfer matrix is simply the identity matrix.

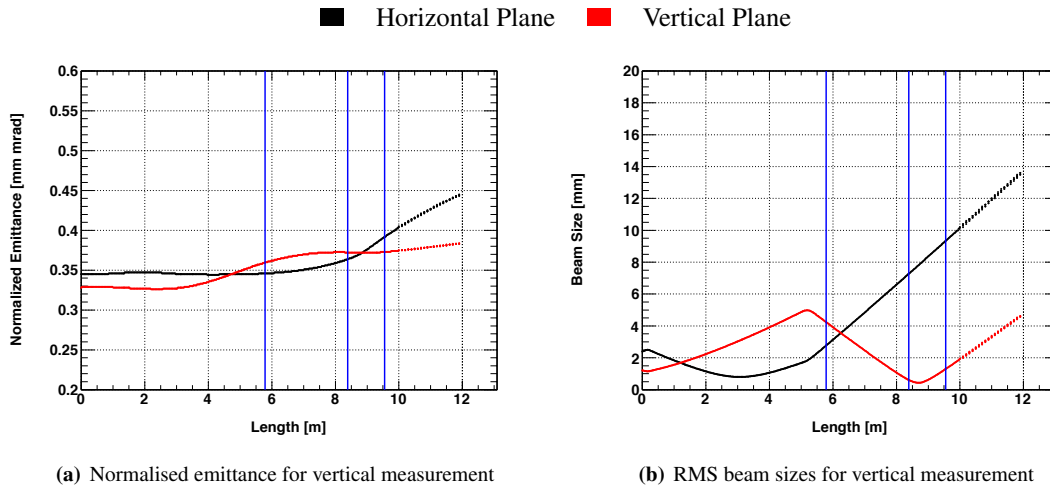


**Figure 6:** Emittance and RMS beam size evolution along the line as simulated with Path for the vertical emittance measurement. The vertical blue lines indicate the three monitor positions.

	Monitor 1 [mm]	Monitor 2 [mm]	Monitor 3 [mm]
horizontal plane	6.911324	0.827755	1.983500
vertical plane	4.229342	0.607148	1.298527

**Table 4:** RMS beam sizes from Path simulations for 65 mA beam current.

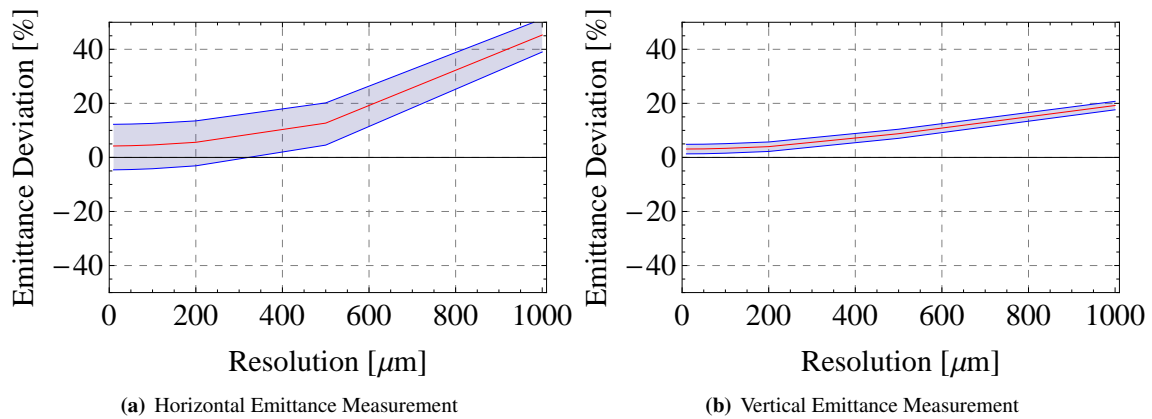


**Figure 7:** Deviation of the reconstructed emittance referred to its reference value at monitor 1 versus different resolution of the beam monitors. The red line indicates the nominal reconstructed value determined for the fitted beam sizes, while the errors band represents the maximum deviations from the nominal value if the fitted beam sizes are systematically varied by their fit parameter error.

In general, the emittance values are best reconstructed the better the resolution of the monitors is, because both curves steeply increase towards the end-point of the curves at 1000  $\mu\text{m}$ . Therefore, smaller resolutions are favored, especially for the second monitor where beam sizes smaller than 1 mm must be measured. A possible explanation for the larger error band for the horizontal measurement is that the beam size histograms, especially for monitor 2 in the horizontal plane, are not entirely Gaussian distributions, as can be seen in Figure 8. Thus, Fig. 8 the Gaussian fit is maybe not the ideal mathematical approximation to the data.

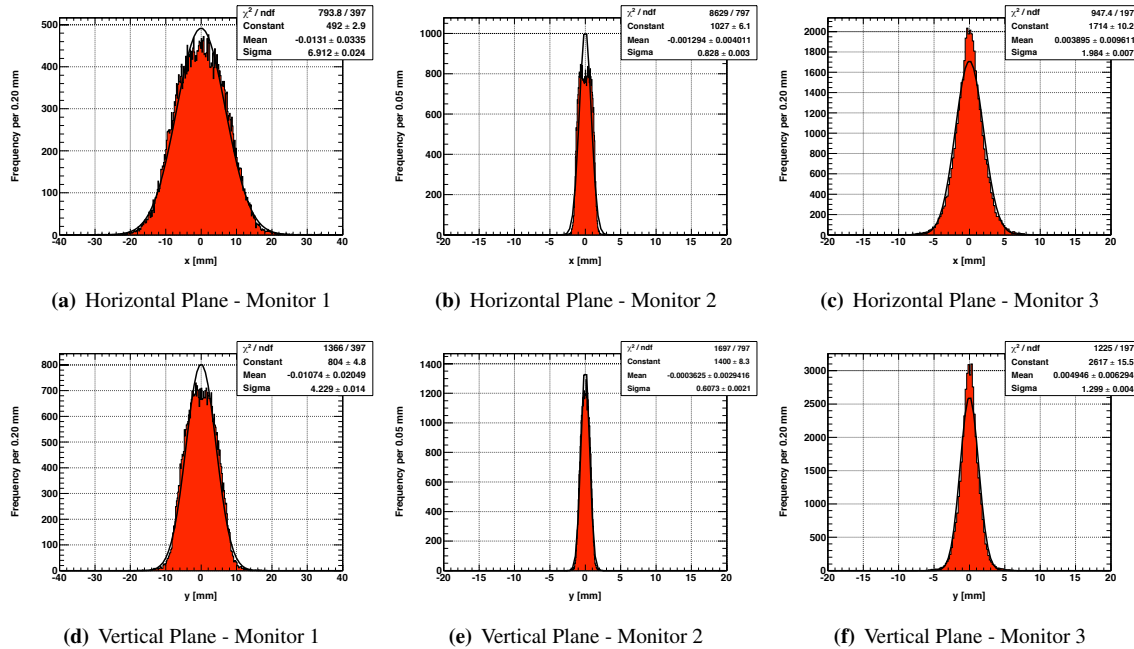


**Figure 8:** Simulation of monitor measurements applying a Gaussian fit to the data. The histogram binning has been chose to be 200  $\mu\text{m}$  for monitors 1 and 3 and 50  $\mu\text{m}$  for monitor 2 (for horizontal and vertical measurement scenario).

In summary, it is proposed to build monitors with a resolution of 200  $\mu\text{m}$  for monitors 1 and 3 and 50  $\mu\text{m}$  for monitor 2 for the emittance measurements in both planes. The following studies are based on this configuration. Although more than a minimally required five measurement points per  $2\sigma$ -beam width can be provided with this assumption, a safety margin for lower beam sizes at reduced beam currents has to be included (Table 6). Tab. 6

### 2.3 Simulation Results for the Nominal Beam

The relative deviations of the beam parameters to their reference values (determined with Path) at the first beam monitor for 65 mA beam current are presented in Table 5 for emittance measurements in both planes. From this it can be seen that the maximum deviation is around 5 %, which satisfies the specification to be  $\leq 10\%$ . The geometric mismatch factor between the reconstructed ellipse and the reference ellipse (from Path) is also negligible. In case the measurement resolution of the central monitor would be downgraded from 50  $\mu\text{m}$  to 100  $\mu\text{m}$ , the relative emittance deviations would increase to +4.83% and +3.47% for the horizontal and vertical measurement, respectively. Tab. 5

As can be seen from Figure 5(a) (black line) and Figure 6(a) (red line), there is emittance growth between the Linac4 exit and monitor 1. Therefore the values determined with the Three-Monitor-Method will have to be corrected by -30.2%/-9.4% (for the horizontal/vertical emittance measurement) to reflect the emittance from Linac4. Fig. 5 Fig. 6

### 2.4 Varying Linac4 Beam Current

An additional test has been performed to evaluate the stability of the method with varying Linac4 beam current. During the commissioning phase of Linac4 it is probable that the source will not yet deliver the design current

	horizontal			vertical		
	$\alpha$	$\beta$ [m/rad]	$\varepsilon$ [mm mrad]	$\alpha$	$\beta$ [m/rad]	$\varepsilon$ [mm mrad]
Reference Values	22.2167	64.3919	0.7417	10.5745	30.1333	0.5936
Reconstructed Values	21.2256	61.5705	0.7759	10.2212	29.1780	0.6131
Relative Deviation	-4.46%	-4.38%	+4.60%	-3.34%	-3.17%	+3.28%
Mismatch Factor $\Delta J$	-0.23%	—	—	-0.14%	—	—

**Table 5:** Results of the reconstruction of the ellipse parameters with the Three-Monitor-Method referred to the reference values read from Path simulations at the first beam monitor for 65 mA beam current. Not only the absolute value, but also the relative deviation compared to the reference values are listed. In addition, for  $\alpha$  and  $\beta$  the mismatch factor  $\Delta J$  is calculated.

of 65 mA. Nevertheless it has to stay possible to measure the transverse emittances with the proposed layout and monitors.

In order to check the implications of varying beam current, additional input beam distributions for 20 and 40 mA are used. With these input parameters, new transfer matrices are calculated with TRACE 3-D and beam sizes determined with Path. The resulting RMS beam sizes at the three monitor positions can be found in Table 6, and the deviations of the beam parameters to their reference values (determined with Path) at the first beam monitor are presented in Table 7 for emittance measurements in both planes and monitor resolutions of  $200\ \mu\text{m}/50\ \mu\text{m}/200\ \mu\text{m}$ . Also under these conditions, the emittance deviations compared to the reference emittance stay at the well acceptable few percent levels.

Tab. 6

Tab. 7

	Monitor 1 [mm]	Monitor 2 [mm]	Monitor 3 [mm]
horizontal plane (40 mA)	6.625788	0.653553	2.082822
vertical plane (40 mA)	4.393178	0.410021	1.659652
horizontal plane (20 mA)	6.016966	0.391629	2.230388
vertical plane (20 mA)	3.847843	0.345254	1.637777

**Table 6:** RMS beam sizes from Path simulations for 40 and 20 mA Linac4 beam current.

	horizontal			vertical			
	$\alpha$	$\beta$ [m/rad]	$\varepsilon$ [mm mrad]	$\alpha$	$\beta$ [m/rad]	$\varepsilon$ [mm mrad]	
40 mA	Reference Values	26.5170	75.2883	0.5832	13.2368	35.8532	0.5384
	Reconstructed Values	25.4825	72.3821	0.6065	12.8756	34.9161	0.5528
	Relative Deviation	-3.90%	-3.86%	+4.00%	-2.73%	-2.61%	+2.67%
	Mismatch Factor $\Delta J$	-0.17%	—	—	-0.09%	—	—
20 mA	Reference Values	26.1810	71.5653	0.5059	11.5801	30.6387	0.4832
	Reconstructed Values	25.8162	70.5931	0.5129	11.4943	30.4307	0.4871
	Relative Deviation	-1.39%	-1.36%	+1.39%	-0.74%	-0.68%	+0.82%
	Mismatch Factor $\Delta J$	-0.03%	—	—	-0.01%	—	—

**Table 7:** Deviation of reconstructed beam parameters with the Three-Monitor-Method referred to the reference values obtained by Path simulations at the first beam monitor for the horizontal and vertical emittance measurement. The geometric mismatch  $\Delta J$  is given as well.

As explained before, the emittances obtained with the Three-Monitor-Method at monitor position 1 will have to be corrected for the emittance growth in the line to reflect the emittance at the Linac4 exit. The corresponding correction factors are -21.6%/-11.4% for 40 mA Linac4 current and -6.2%/-3.6% for 20 mA beam current for the horizontal/vertical emittance measurement, respectively.

As an additional test the emittance has been calculated with all combinations of transfer matrices and beam sizes (see Table 8). For all possible combinations the emittance deviations do not exceed 5%. In principle it would be

Tab. 8

possible to use the transformer reading to provide transfer matrices from a look-up table corresponding to the beam current range present. But seen the results, this should not be necessary.

	Transfer matrix at				Transfer matrix at		
	20 mA	40 mA	65 mA		20 mA	40 mA	65 mA
BS 20 mA	1.39%	1.11%	0.39%	BS 20 mA	0.82%	0.51%	0.11%
BS 40 mA	2.00%	4.00%	3.00%	BS 40 mA	2.25%	2.67%	2.56%
BS 65 mA	3.00%	5.37%	4.60%	BS 65 mA	2.01%	3.07%	3.28%

**Table 8:** This matrix shows emittance deviations between the calculated emittances and the Path reference values for 20, 40 and 65 mA beam current (left for the horizontal, right for the vertical measurement). In the diagonal the correctly calculated values are represented for both cases, where the transfer matrices (TM) and beam sizes (BS) have been taken for the same beam current. The other elements allow to estimate the error that would be made in case the transfer matrices would not be adapted to the corresponding beam current.

## 2.5 Varying Longitudinal Input Parameters

The Linac4 dump line is a very challenging location for an emittance measurement, not only because of the strong space charge forces at 160 MeV and the emittance growth along the line, but also due to the transition between a controlled longitudinal regime (bunched beam) to an unbunched beam in the transfer line, where longitudinal space charge forces are uncompensated. Therefore another test has been made where the transfer matrices were recalculated with TRACE 3-D for approximately half of the longitudinal emittance (400 deg keV) at the most challenging case of nominal beam current (65 mA). Using the original beam size measurements from Path, the deviations of the calculated emittance at monitor 1 with respect to the reference emittance were determined and are shown in Table 9. The errors are in the same range as for the nominal configuration (see Table 5), indicating that changes in the longitudinal plane up to 50% seem not to be of a concern.

Tab. 9  
Tab. 5

Transfer line coefficient	$C_1$	$S_1$	$C_2$	$S_2$	$C_3$	$S_3$
horizontal	1.0	0.0	1.013804	2.615805	1.063622	3.898374
vertical	1.0	0.0	1.036344	2.639423	1.119972	3.983304
	horizontal			vertical		
Emittance Deviation $\Delta\varepsilon_{\text{rel}}$	3.73%			2.99%		

**Table 9:** Transfer matrix coefficients and emittance deviations for half the longitudinal emittance and 65 mA beam current.

Additional systematic studies have been made to show the robustness of the method with the Linac4 beam for the LBE line emittance measurement. These studies should also be valid for the Linac4 dump line setup. Please refer to chapter chapter 3.4 for more details.

Chp. 3.4

## 2.6 Limitations

It has to be stated that the Three-Monitor-Method works only if the transfer matrices are precisely known. This will not be the case during the Linac4 commissioning phase. The situation has been studied where alpha and beta would have only half their nominal value combined with half the longitudinal emittance at nominal beam current. In this situation, using either the newly calculated transfer matrices with the original beam size values or the original transfer matrices with new beam sizes estimated from TRACE 3-D (this case would approach better the real situation), the error in the emittance calculation can reach 30% for the horizontal measurement and 7% for the vertical measurement. A change of 50% in alpha and beta seems to be realistic during the Linac4 commissioning phase [7], even though a measurement of alpha and beta is foreseen already during the first phase of Linac4 commissioning at the 12 MeV movable diagnostics bench after Linac4 tank 1.

Ref. [7]

Therefore it has to be concluded that with the proposed layout in the Linac4 dump line using the Three-Monitor-Method the emittance of the Linac4 beam can be determined during normal Linac4 operation, once the Linac4 output beam parameters will be approximately stable and known. During Linac4 commissioning phase the

Ref. [8] method would result in too large errors. Nevertheless the setup could be used to measure the emittance also during the commissioning phase, applying an iterative calculation method as described in reference [8].

### 3 LBE Line

Ref. [9] The LBE line in its present design is used to measure the emittance of the beams from the CERN Linac2 (protons at 50 MeV) and Linac3 (heavy ions at 4.2 MeV/nucleon) accelerators. It is based on a phase space scan by sampling slices of a beam pulse with a slit and measuring its image further downstream with a SEM<sup>6</sup> grid [9]. Instead of upgrading the elements of the line it is studied if the simpler Three-Monitor-Method would give satisfying results, because from its principle the measurement is less prone to errors and the cost for the upgrade could be kept lower.

#### 3.1 LBE Line Simulations

Ref. [10, 11] Despite the need to upgrade the LBE line for Linac4 operation, its functionality for heavy ion operation must still be preserved. Therefore, it is planned to fit the required equipment for the Three-Monitor-Method into the present design, meaning that the empty spaces in the LBE line have been identified at first. As the beam must form the demanded beam waist for applying the Three-Monitor-Method, only empty zones behind the two quadrupole magnets can be considered because both magnets are needed for beam manipulation. In Figure 9 a schematic picture created from the technical drawings of the LBE line [10, 11] is shown.

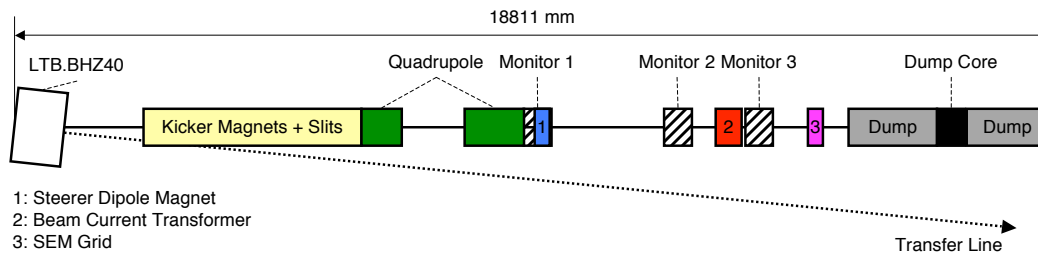


**Figure 9:** Schematic layout of the LBE line. The positions of the three proposed beam monitors are marked with striped boxes. The LTB.BHZ40 is a dipole magnet, bending the beam from the transfer line to the PS Booster into the LBE line (bending angle: 100 mrad). Kicker magnets, slit objects and SEM grid are exclusively necessary for heavy ion operation.

The potential positions of the three monitors are marked with striped boxes. It can be seen that the first monitor overlaps with the steerer dipole magnet, which must be shifted slightly further downstream. Additionally, for a controlled removal of the beam from the line a beam dump must be installed at the end of the line, so that the overall length will be about 18.8 m.

Tab. 10 Starting from the beam input parameters right in front of the LTB.BHZ40 dipole magnet as presented in Table 10, the LBE line is simulated with the TRACE 3-D code (refer to Appendix B for the configuration file). Independently for the measurement of the horizontal and vertical emittance, a set of field gradient values for the two quadrupole magnets can be found, such that between the exit of the second quadrupole and the end of the line the beam waist is formed<sup>7</sup>. These values are also mentioned in Table 10.

Tab. 11 The three positions in the empty spaces are identified such that the angles of the horizontal and vertical phase space ellipses differ by about 60° between adjacent positions. The positions as well as the beam parameters at these three locations are quoted in Table 11. All lengths in the LBE line – also throughout the rest of this chapter – are referred to the beginning of the line, which is at the entrance of the LTB.BHZ40 dipole magnet (distance 0). In order to cope with a future technical realization of this setup a length of 500 mm is reserved per monitor, which represents a typical vacuum tank with a single beam monitor at its mid-position. Additionally, the setup can be tuned so that for emittance measurements in both transverse phase space planes the same monitor positions can be used. Only the field gradients of the quadrupole magnets must be set separately.

<sup>6</sup>Secondary Emission Monitor.

<sup>7</sup>The present quadrupole magnets only provide field gradients of less than 1.3 T/m so that they must be replaced for the emittance measurement with the Three-Monitor-Method.

	$\alpha$	$\beta$	$\varepsilon(1\sigma)$
horizontal	-0.211	5.357 mm/mrad	0.657 mm mrad
vertical	2.520	22.978 mm/mrad	0.749 mm mrad
longitudinal	15.209	4.038 deg/keV	388.833 deg keV
	Quad 1	Quad 2	
horizontal plane	0.60 T/m	-1.90 T/m	
vertical plane	-2.00 T/m	-2.25 T/m	

**Table 10:** Input parameters for the LBE line simulations with TRACE 3-D and settings of the quadrupole magnets for the emittance measurements in the horizontal and vertical plane. The input beam parameters have been provided by the Linac4 beam dynamics working group.

	Monitor Position [mm]	$\alpha$	$\beta$ [mm/mrad]	$\varphi$	$r(1\sigma)$ [mm]	$\varepsilon(1\sigma)$ [mm mrad]
horizontal plane	9536	8.273	22.530	159.80°	3.865	0.6830
	12081	0.450	0.395	99.39°	0.512	0.6828
	13529	-3.971	5.486	36.50°	1.907	0.6828
vertical plane	9536	2.399	7.117	161.06°	2.309	0.7490
	12081	-0.010	1.084	93.49°	0.901	0.7490
	13529	-1.360	3.065	25.94°	1.515	0.7490

**Table 11:** Positions of the beam monitors, ellipse parameters and expected beam sizes at the three beam monitor positions. All values are taken from TRACE 3-D simulations. The distances referred to the first monitor are 2545 mm for monitor 2 and 3993 mm for monitor 3.

From the beam parameters the difference of the phase space ellipse angles between the three monitor positions can be calculated. These results coincide reasonably well with the theoretical value of 60° for optimal sampling of the beam ellipse.

$$\begin{aligned}
\Delta\varphi_{12}^{\text{hor}} &= 60.41^\circ & \Delta\varphi_{12}^{\text{ver}} &= 67.57^\circ \\
\Delta\varphi_{23}^{\text{hor}} &= 62.89^\circ & \Delta\varphi_{23}^{\text{ver}} &= 67.55^\circ
\end{aligned}
\tag{12}$$

Furthermore, the value of the transverse emittance is approximately constant along the entire measurement section as well. This is depicted in Figure 10 for the evolution of the normalized emittance values along the LBE line. The deviations are only at the level of 0.1%. In addition, it can be seen that the two planes are sufficiently decoupled because the virtual emittance increase at the beginning of the line in the horizontal plane, correlated with the induced dispersion along the length of the *horizontal* LTB.BHZ40 dipole magnet, cannot be observed in the vertical plane.

The reference point for the measurement is placed at the first monitor, at which the values for emittance and ellipse parameters are reconstructed. This has the advantage that distortions of the quadrupole fields are explicitly not included in the transfer matrix elements, which must be respected if the reference point lies in front of the quadrupole magnets. Thus, the transfer matrices between the first and the two other monitors are determined from the TRACE 3-D code (Table 12). They are used to obtain the elements of the matrix  $M$  in equation 8.

	$C_1$	$S_1$	$C_2$	$S_2$	$C_3$	$S_3$
horizontal plane	1.0	0.0	1.005602	2.551484	1.022053	4.035342
vertical plane	1.0	0.0	1.020589	2.559032	1.041871	4.031970

**Table 12:** Cosine- and sine-like elements of the transfer matrices between the reference point at the first monitor and the three monitor positions.

Being the reference point, the values for  $C_1$  and  $S_1$  represent the unit matrix. If no electromagnetic interactions



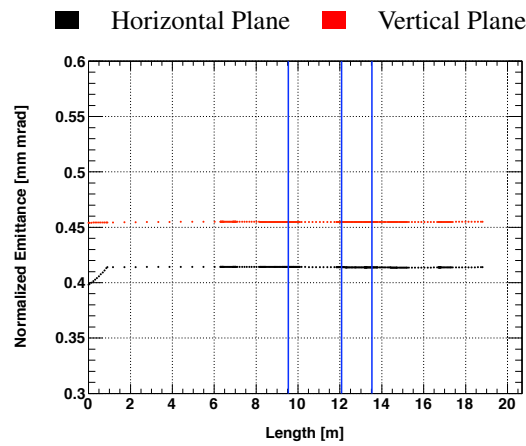


**Figure 10:** Horizontal and vertical emittance (normalized) evolution along the LBE line. The vertical blue lines indicate the positions of the beam monitors.

would be present, the cosine-like elements  $C_2$  and  $C_3$  would be equal to unity, whereas the sine-like  $S_2$  and  $S_3$  elements would just represent the distance of the second and third monitor to the first one (in meters). Thus, the deviations from these ideal values allow for a rough estimate of existing space charge effects.

### 3.2 Reconstruction of Transverse Emittance Values and Phase Space Ellipses

Having simulated the measurement line with TRACE 3-D the beam sizes necessary for solving equation 8 are determined with the Path simulation program. In Figure 11 the evolution of the beam size along the LBE line is illustrated, while in Table 13 the reference beam sizes for the horizontal and vertical measurements at the three monitor positions from Path simulations are summarized.

Fig. 11  
Tab. 13

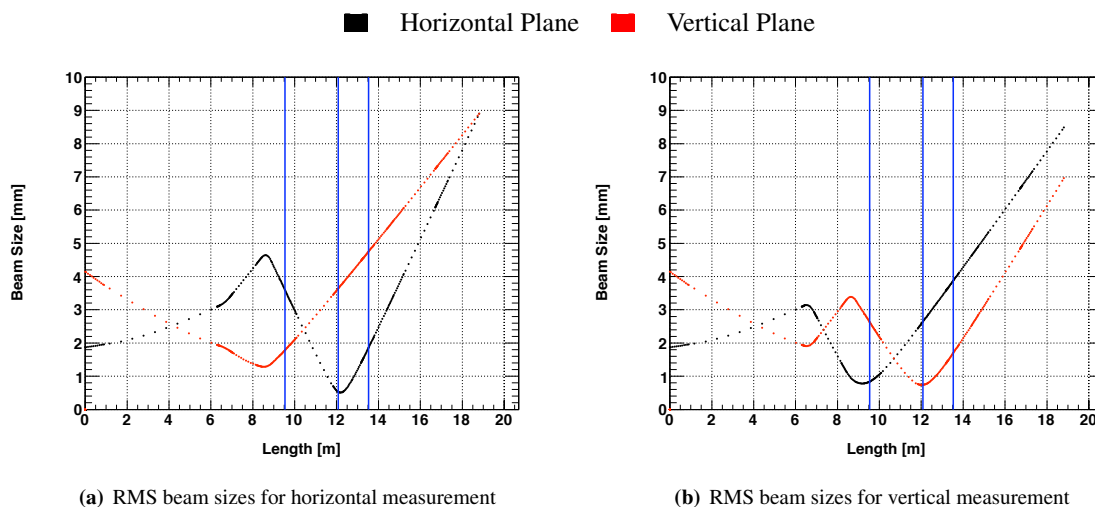


**Figure 11:** Evolution of RMS beam size along the LBE line for the measurement of the horizontal (left) and vertical (right) emittance. The positions of the three beam size monitors are pointed out by the vertical blue lines.

It is obvious that these values cannot be experimentally measured to the above-given precision. Therefore, as described in chapter 1.3, the data are filled into histograms with bin widths adapted to potential monitor resolutions and the beam size is deduced from a Gaussian fit. In Figure 12 the deviation of the reconstructed emittance from its reference value is depicted for various resolution values. The red line is the nominal reconstructed value for the fitted beam size according to equation 8 without contemplating the fit errors. For the error band all combinations of three beam sizes varied by plus and minus their fit parameter errors are used to get eight reconstructed emittance values. The maximum and minimum values of this set are taken as the upper and

Chp. 1.3  
Fig. 12

	Monitor 1 [mm]	Monitor 2 [mm]	Monitor 3 [mm]
horizontal plane	3.824616	0.510254	1.946681
vertical plane	2.252501	0.906302	1.541280

**Table 13:** RMS beam sizes at the monitor positions from Path simulations.

lower boundaries of the band per data point.

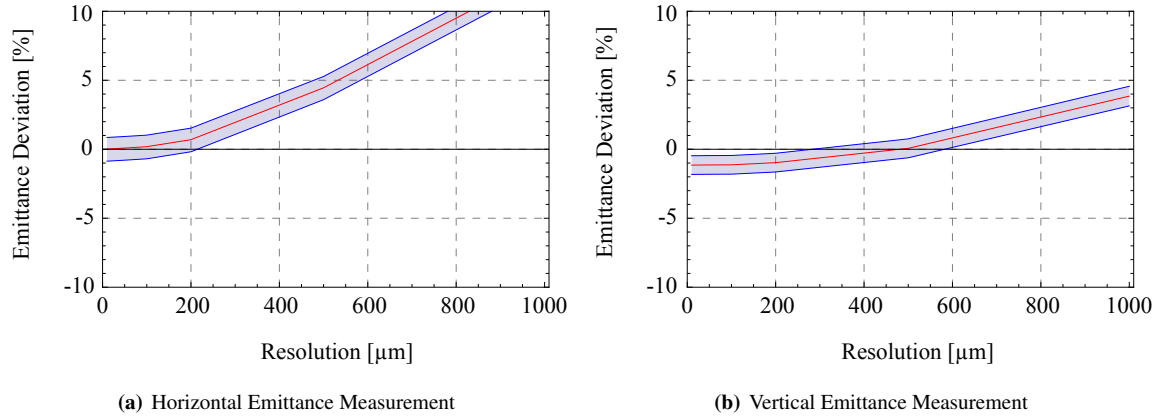


**Figure 12:** Deviation of the reconstructed emittance referred to its reference value at monitor 1 versus different resolution of the beam monitors. The red line indicates the nominal reconstructed value determined for the fitted beam sizes, while the errors band represents the maximum deviations from the nominal value if the fitted beam sizes are systematically varied by their fit parameter error.

In general, the emittance values are best reconstructed the better the resolution of the monitors is. Both curves steeply increase towards the end-point of the curves at 1000  $\mu\text{m}$ . The effect is more pronounced for the horizontal plane, because the very small beam size at monitor position 2 requires a fine resolution to get sufficient data points for the fitting algorithm. On the other hand for the vertical plane the best result is not achieved for the highest resolution. However, it is assumed that this is a systematic effect, which is related to the fact that the phase space distribution is not entirely elliptical and the fitted distributions are therefore not simply Gaussian. As an example, in Figure 13 the phase space distributions at the reference monitor 1 are illustrated.

Fig. 13

In summary, driven by the resolution requirements for the horizontal plane and influenced through searching for a technically homogenous solution including the Linac4 dump line, it is proposed to build monitors with a resolution of 200  $\mu\text{m}$  for monitors 1 and 3, and with a resolution of 50  $\mu\text{m}$  for monitor 2 for both measurement planes. The dedicated histograms including the Gaussian fit are revealed in Figure 14. Unless differently mentioned, this resolution configuration is chosen as default for the following studies. Although more than a minimally required five measurements per  $2\sigma$ -beam width are provided, a safety margin for lower beam sizes at reduced beam currents is included.

Fig. 14

### 3.3 Simulation Results for the Nominal Beam

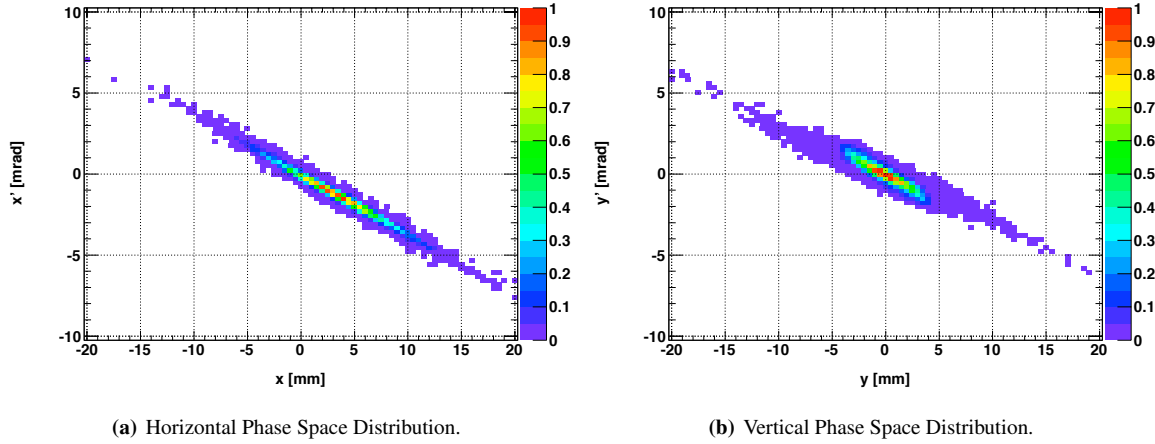
The results of the reconstruction of the ellipse parameters for the nominal 65 mA beam with the Three-Monitor-Method in comparison to their reference values at the first beam monitor are presented in Table 14.

Tab. 14

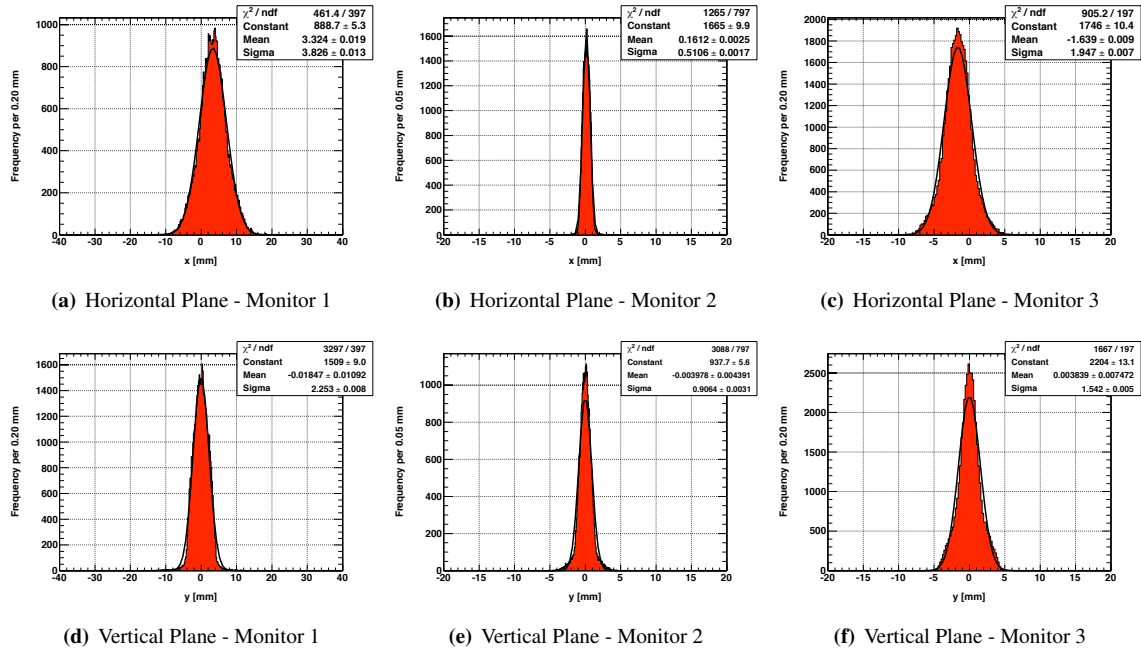
The parameter error on the fitted beam sizes leads to a typical uncertainty of 1 % for the reconstructed emittance, in reasonable accordance with the width of the error band of Figure 12.

Fig. 12

If a typical maximum target deviation of  $\pm 10\%$  is not exceeded, the measurement is considered as reliable. Hence, for both transverse planes the ellipse parameters are reasonably well reconstructed by the Three-Monitor-Method, provided that systematic errors can be controlled, too, for which a margin is still available. But it must be emphasized that a worse resolution, especially for the second beam monitor, degrades the obtained results. Decreasing the measurement resolution for the central monitor from 50  $\mu\text{m}$  to 100  $\mu\text{m}$  with the nominal beam



**Figure 13:** Reference phase space distributions at the location of monitor 1 in the horizontal (left) and vertical (right) plane with quadrupole settings used during horizontal emittance measurement (left) and vertical measurement (right).



**Figure 14:** Simulation of monitor measurements with Gaussian fit to the data. The applied resolutions are  $200\ \mu\text{m}$  for monitors 1 and 3 and  $50\ \mu\text{m}$  for monitor 2 (for both planes).

	horizontal			vertical		
	$\alpha$	$\beta$ [m/rad]	$\varepsilon$ [mm mrad]	$\alpha$	$\beta$ [m/rad]	$\varepsilon$ [mm mrad]
Reference Values	7.9235	21.4351	0.6824	2.2845	6.7696	0.7495
Reconstructed Values	7.9052	21.3262	0.6832	2.3004	6.7594	0.7414
Relative Deviation	-0.23%	-0.51%	+0.12%	+0.70%	-0.15%	-1.08%
Mismatch Factor $\Delta J$		-0.05%	—		-0.04%	—

**Table 14:** Results of the reconstruction of the ellipse parameters with the Three-Monitor-Method referred to the reference values read from Path simulations at the first beam monitor. Not only the absolute value, but also the relative deviation compared to the reference values are listed. In addition, for  $\alpha$  and  $\beta$  the mismatch factor  $\Delta J$  is calculated. A dispersion correction is not applied, because no appropriate reference values to assess the quality of the reconstruction are available.

current almost doubles the emittance deviation for the horizontal measurement, but leaves it practically constant for the measurement in the vertical plane. The implementation of the LBE line should aim at measurement precisions as low as  $50\ \mu\text{m}$ , in particular in view of possible decreased beam current, which seems to be technically feasible [5].

Ref. [5]

### 3.4 Systematic Studies

It is only possible to choose the Three-Monitor-Method for emittance and ellipse parameter measurements if the solution of the equation system is robust to deviations from the above-described optimal measurement scenario. In this paragraph the stability of the solution itself is tested and the effect of systematic variations of the beam line parameters investigated.

#### Stability of the Beam Parameters when Iteratively Solving the Equation System

In order to assess the robustness of the reconstructed beam parameters the equation system is iteratively solved. The idea behind this reiteration is that the elements of the transfer matrices between the different monitors depend on the beam parameters if space charge effects are respected. Having found a solution of the equation system, in the next step the transfer matrix elements are recalculated, inserting the just reconstructed parameters into the TRACE 3-D simulations. For the longitudinal plane and the transverse plane not under consideration the original input values are taken. Then, the equation system is solved again, while the beam size measurements are left untouched. In this manner the actual and the next reconstruction step are connected. In Figure 15 the results of this iterative process for four reiterations are graphically shown. On the left vertical axes the absolute emittance values are given and on the right vertical axes the relative deviations to the reference value.

Fig. 15

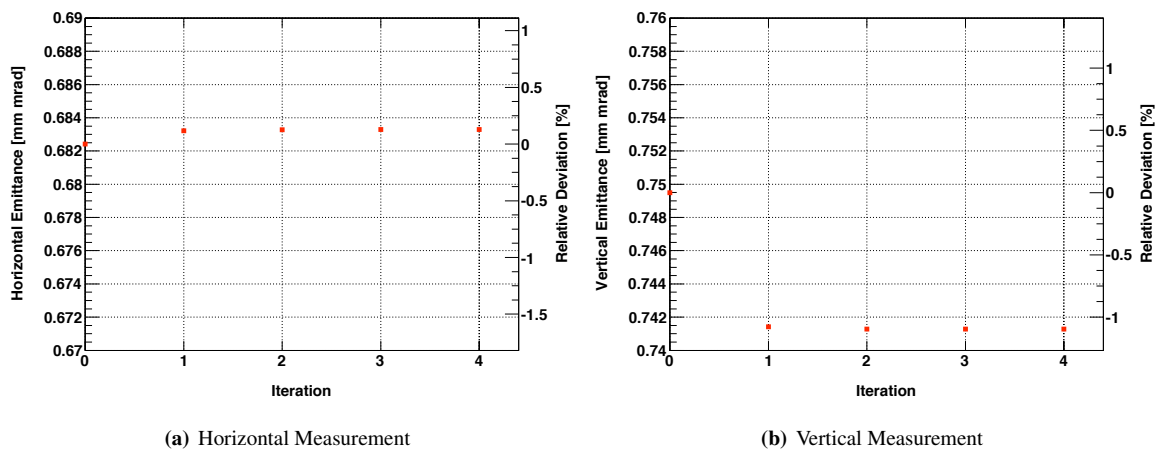


**Figure 15:** Iteratively reconstructed emittance values. The entry for iteration 0 shows the reference value obtained from the Path simulation code at monitor 1.

The value at iteration 0 is the reference value at monitor 1 from Path, and in both transverse planes almost the entire experimental deviation from this value arises when the equation system is solved for the first time (iteration 1). After that, the iteratively calculated matrix elements, which deviate from step to step by a few per mille at maximum, do not significantly influence the results. The relative difference for the emittance change is highest from iteration 1 to 2 –  $\mathcal{O}(10^{-3}\%)$  – and decreases even further to  $\mathcal{O}(10^{-6}\%)$  in iteration 4. Hence, the initial solution converges very rapidly and provides a good estimate of the emittance value. Similar results are valid for the parameters  $\alpha$  and  $\beta$  in both transverse planes.

#### Errors on Quadrupole Field-Gradients and Beam Monitor Positions

The systematic error due to possible deviations in the settings of the field gradient of the quadrupole magnets and on the alignment precision of the beam monitors is estimated in the following way. Conservatively, for both quadrupole magnets the nominal field gradient is varied by  $\pm 1\%$ , while the positions of the beam monitors are

shifted by  $\pm 5$  mm, so that in total five elements are affected with two variations per element. Per element the greater deviation of the two is chosen (worst case), and in the end the total systematic error is the square root of the quadratic sum of these five values.

Then, there are two ways to study the effects of these systematic errors. At first, the equation system is solved assuming that the transfer matrices remain unchanged while at the same time the beam sizes are newly determined with the systematically modified beam line layout. This gives an estimate on the direct systematic error on the beam parameter measurements due to alignment and optical errors. On the other hand the nominal beam sizes of Table 13 are chosen, but new transfer matrix elements are extracted from TRACE 3-D simulations. So the uncertainty of the measurement due to errors on the transfer matrix elements can be estimated assuming a mismatch between the real setup of the LBE line and the implementation in the simulation.

Tab. 13

Hence, when keeping the transfer matrix elements constant (more realistic case), the systematic errors are

$$\begin{aligned}\Delta\varepsilon_{\text{rel}}^{\text{hor}} &\approx 0.69\% \\ \Delta\varepsilon_{\text{rel}}^{\text{ver}} &\approx 0.21\%\end{aligned}\quad (13)$$

and when keeping the beam sizes constant

$$\begin{aligned}\Delta\varepsilon_{\text{rel}}^{\text{hor}} &\approx 0.65\% \\ \Delta\varepsilon_{\text{rel}}^{\text{ver}} &\approx 0.18\%.\end{aligned}\quad (14)$$

For the parameters  $\alpha$  and  $\beta$  results up to significantly less than 2% are obtained. Hence, the systematic error due to magnetic field errors of the quadrupole magnets, alignment errors of the beam size monitors and uncertainties in the transfer matrix elements are controllable.

### Variation of Beam Input Parameters

The results obtained for the Three-Monitor-Method coincide quite well with the reference values because the matrix elements and beam sizes are deduced for the same set of input parameters. However, it is questionable if the method still gives reliable results if matrix elements and beam sizes are created for different beam input parameters. This scenario could happen if later on in the experiment the beam parameters at the beginning of the LBE line are different from what has been assumed for these simulations. In principle, it is equivalent for this problem if new beam size are measured and the nominal matrix elements are used, or if the nominal beam sizes are kept and new matrix elements are determined.

In order to test the stability of the method, at first the longitudinal emittance is set to half of its nominal value, i.e.  $\varepsilon_L^{1\sigma} = 194.4$  deg keV. This resembles a beam, which is compressed in longitudinal direction, so that the space charge density increases and repulsive space charge forces become more relevant. The elements of the transfer matrix are newly determined and the equation system is solved with the nominal beam size values. The result in Table 15 indicates that this is acceptable because the reconstructed values deviate by the same amount from the reference values as for the nominal solution.

Tab. 15

	horizontal			vertical		
	$\alpha$	$\beta$	$\varepsilon$	$\alpha$	$\beta$	$\varepsilon$
Relative Deviation	-0.04%	-0.46%	+0.07%	+1.30%	+0.15%	-1.37%
Mismatch Factor $\Delta J$	-0.11%	—	—	-0.07%	—	—

**Table 15:** Results of the reconstruction of the ellipse parameters with the Three-Monitor-Method referred to the reference values read from Path simulations at the first beam monitor. In this case the parameters are determined using nominal beam sizes but transfer matrices for beams with longitudinal emittance set to half of its nominal value, i.e.  $\varepsilon_L^{1\sigma} = 194.4$  deg keV. All other parameters have been left untouched.

Then, still for  $\varepsilon_L^{1\sigma} = 194.4$  deg keV, the transverse beam parameters at the first monitor have been modified. For the horizontal measurement the values for  $\alpha_H$ ,  $\beta_H$  and  $\beta_V$  are halved and  $\alpha_V$  is set to zero in TRACE 3-D, while for the vertical measurement  $\beta_H$ ,  $\alpha_V$  and  $\beta_V$  are halved and  $\alpha_H$  becomes zero. With these parameters new transfer matrices are determined and new beam sizes are estimated, the latter exceptionally from TRACE 3-D simulation because of the lack of proper Path data. Afterwards the beam parameters are calculated mixing

(1) the new transfer matrix elements with the nominal Path beam sizes, and (2) the nominal transfer matrices with the new beam sizes from TRACE 3-D. The results are summarized in Table 16.

Tab. 16

		horizontal			vertical		
		$\alpha$	$\beta$	$\varepsilon$	$\alpha$	$\beta$	$\varepsilon$
(1)	Relative Deviation	-0.67%	-0.44%	+0.04%	+4.39%	<0.002%	-1.23%
	Mismatch Factor $\Delta J$	-0.78%	—	—	-1.01%	—	—
(2)	Relative Deviation	-47.04%	-46.64%	-2.97%	-46.10%	-44.77%	0.23%
	Mismatch Factor $\Delta J$	-40.95%	—	—	-36.46%	—	—

**Table 16:** Results of the reconstruction of the ellipse parameters with the Three-Monitor-Method referred to the reference values read from Path simulations at the first beam monitor. For both results the beam parameters have been manipulated to half of their nominal values at the first monitor, and the longitudinal emittance is set to  $\varepsilon_L^{1\sigma} = 194.4$  deg keV. In case (1) new transfer matrices are used, and in case (2) new beam sizes are estimated with TRACE 3-D.

For the case (1) it can be concluded that even this considerable modification of beam parameters has only a limited influence on the precision of the reconstructed values, because the matrix elements only vary by a few percent. In case (2) the large deviations for  $\alpha$  and  $\beta$  only mimic a wrong result because the reference values are still taken as the nominal beam parameters. Therefore, actually the correct input parameters (half of the nominal values) instead of the reference values are approximately reproduced. This is further emphasized by the reconstructed emittance value. It is very close to all previously cited results, but one should be cautious with the absolute value itself. The beam sizes are only estimated from TRACE 3-D and systematic effects due to choosing different programs for beam size determinations must be included as well.

### 3.5 Measurement with more than Three Monitors

As it has been explained in chapter 1.1 the equation system can be solved numerically if it becomes overdetermined when the beam sizes are measured at more than three positions. In order to investigate the effect of these additional monitors, two more are virtually installed in the LBE line, one before and one behind the beam waist, and the third monitor is shifted downwards by 199 mm. As before, all monitors serve to measure beam sizes in both transverse planes. The beam data equivalent to Table 11 are shown in the following table.

Tab. 11

	Monitor Position [ mm ]	$\alpha$	$\beta$ [ mm/mrad ]	$\varphi$	$r(1\sigma)$ [ mm ]	$\varepsilon(1\sigma)$ [ mm mrad ]
horizontal plane	9536	8.273	22.530	159.80°	3.865	0.6826
	11331	2.740	2.786	133.60°	1.359	0.6827
	12081	0.450	0.395	99.39°	0.512	0.6827
	12631	-1.226	0.822	66.11°	0.738	0.6827
	13728	-4.581	7.188	32.87°	2.183	0.6827
vertical plane	9536	2.399	7.117	161.06°	2.309	0.7490
	11331	0.689	1.593	147.92°	1.092	0.7490
	12081	-0.010	1.084	93.49°	0.901	0.7490
	12631	-0.521	1.377	33.27°	1.015	0.7490
	13728	-1.547	3.644	24.38°	1.652	0.7490

**Table 17:** Positions of the beam monitors, ellipse parameters and expected beam sizes for the five monitor positions.

There are several advantages of having more than three monitors. Obviously, it is desirable to already have installed spare parts if one of the absolutely required three monitors breaks down. This allows for more freedom of maintenance planning in a zone of radioactive activation. From the physics point of view the measurement – mathematically the equation system – can be extended such that more than just the basic phase space parameters  $\alpha$ ,  $\beta$ , and  $\varepsilon$  can be determined. In theory, five monitors allow in addition for measurements of dispersion and momentum spread. Therefore, the measurement program can potentially be extended without intervening in the beam line. The other option to obtain the additional beam size measurements by varying the quadrupole field

gradients and record values at the already existing three locations is less favored for several reasons. At first, the transfer matrices become explicitly dependent on the quadrupole parameters, and so fringe fields must be accounted for, which are only approximatively described by the matrix formalism. Therefore, this uncertainty cannot be excluded anymore. Secondly, a single quadrupole setting scenario leads to a certain set of expected beam sizes, so that the resolutions of the beam monitors can be optimized to these values. But if the quadrupole settings are modified to generate more measurement points, the values can change by an order of magnitude, for which the monitors are not tuned anymore. At last, for different field gradients the beam steering must also be adapted to the new beam evolution. This does not become necessary if only one quadrupole setting is required when the number of beam monitors is increased.

For the chosen setup with five monitors the following differences between the orientation angles of the phase space ellipses are derived from the beam parameters

$$\begin{aligned}
 \Delta\varphi_{12}^{\text{hor}} &= 26.20^\circ & \Delta\varphi_{12}^{\text{ver}} &= 13.14^\circ \\
 \Delta\varphi_{23}^{\text{hor}} &= 34.21^\circ & \Delta\varphi_{23}^{\text{ver}} &= 54.43^\circ \\
 \Delta\varphi_{34}^{\text{hor}} &= 33.28^\circ & \Delta\varphi_{34}^{\text{ver}} &= 60.22^\circ \\
 \Delta\varphi_{45}^{\text{hor}} &= 33.24^\circ & \Delta\varphi_{45}^{\text{ver}} &= 8.89^\circ
 \end{aligned} \tag{15}$$

It can be observed that in the horizontal plane the differences are approximately equidistant, but in the vertical plane this is not achieved. In the latter case the phase space distribution is almost circular and the minimum of the vertical beta-function is very flat. Thus, a small variation of the position of observation results immediately in a large angular shift. Finally, the decision on the monitor positions is mainly influenced by space constraints and it is desired that both transverse beam sizes can be measured with monitors at the same locations. In this case, the selected positions are rather optimized for the horizontal than for the vertical plane.

The resolutions of the five monitors are again adapted to the expected beam sizes. For the outermost positions the beam sizes do not or only marginally change, so that the resolution is kept at 200  $\mu\text{m}$ . The resolution for the inner monitor 3 is chosen to be 50  $\mu\text{m}$ , because the beam size at the mid-position for the horizontal measurement is still only 0.5 mm for the maximum beam current. In addition, the beam size for monitors 2 and 4 increase by only about 20% in the vertical case compared to monitor 3, so that a choice of 50  $\mu\text{m}$  resolution for the mid-monitor immediately leads to the same resolution for these two monitors to get homogenous measurements.

The results for the five monitor setup are presented in Table 18.

Tab. 18

	horizontal			vertical		
	$\alpha$	$\beta$ [m/rad]	$\varepsilon$ [mm mrad]	$\alpha$	$\beta$ [m/rad]	$\varepsilon$ [mm mrad]
Reference Values	7.9235	21.4351	0.6824	2.2845	6.7696	0.7495
Reconstructed Values	7.8363	21.1497	0.6890	2.2937	6.7500	0.7428
Relative Deviation	-1.10%	-1.33%	+0.97%	+0.40%	-0.29%	-0.90%
Mismatch Factor $\Delta J$		-0.05%	—		-0.03%	—

**Table 18:** Results of the reconstruction of the ellipse parameters with the Five-Monitor-Method referred to the reference values read from Path simulations at the first beam monitor. Not only the absolute value, but also the relative deviation compared to the reference values are listed. In addition, for  $\alpha$  and  $\beta$  the mismatch factor  $\Delta J$  is calculated. A dispersion correction is not applied, because no appropriate reference values to assess the quality of the reconstruction are available.

Tab. 14  
Tab. 18

Comparing the results of the Three-Monitor-Method (Table 14) and Five-Monitor-Method (Table 18) it can be seen that the results for the horizontal measurement become slightly worse, while for the vertical measurement the results improve a bit. However, in general no significant change of the results can be observed when adding the additional monitors.

At last, another stability test of the Three-Monitor-Method can be performed with the five measurement points. All ten potential three monitor combinations out of the five monitor samples are evaluated, the ellipse parameters reconstructed and compared to the reference value. Here only key conclusions are summarized. Detailed numerical results are listed in Appendix C.

- From the majority of solutions one obtains similar results to the optimal Three-Monitor-Method measurement. Hence, even if the phase space ellipses are scanned with different orientations compared to the

optimal one, the beam parameters are still reliably reconstructed. The deviations are at the order of 1% or even below, but in any case far lower than the target limit of 10%.

- The largest deviations occur when two phase space ellipses are taken into account, which lie very close to each-other.
- Geometrically, the combination of monitors 1, 3, and 5 approaches most closely the Three-Monitor-Method measurement, only the position of the third monitor being slightly shifted. As the reconstruction results are not identical but very close, the stability of the method is further proven.
- A global comparison between all ten combinations shows that the combination of monitors 1, 3, and 5 is a good compromise for both transverse planes and all ellipse parameters, even if better values for single parameters in any of the two planes can be obtained by selecting another combination.

In summary, it is proposed to install three monitors in the LBE line for the measurement of the transverse emittance values at positions 9536 mm, 12081 mm and 13529 mm from the entrance of LTB.BHZ40.

## 4 Summary and Conclusions

In this report the option to measure both transverse emittance values with the Three-Monitor-Method has been tested. If at least three beam size measurements and the transfer matrix between the measurement stations are known, the phase space ellipse parameters  $\alpha$ ,  $\beta$ , and  $\varepsilon$  can be calculated from a linear equation system.

This method has been applied to the Linac4 160 MeV H<sup>-</sup>-beam shortly after the Linac4 exit in the Linac4 dump line and close to the injection point into the PS Booster in the LBE line. A layout proposal has been provided, and in general it could be shown that the method is applicable for both lines. Due to multiple scattering and stripping, the three measurements will have to be performed successively with a maximum beam duration of 100  $\mu$ s to avoid damage to the screens and dumps.

The non-linear corrections due to space charge effects in this linear approach are only of the order of a few percent if adequate resolutions for the three beam size monitors are chosen. In the present case a resolution of 200  $\mu$ m for the two outer monitors and 50  $\mu$ m for the central monitor is found to be reasonable. This choice already respects that beam sizes will be smaller for reduced Linac4 beam currents.

There is no need for more than three monitors because the gain in measurement precision is not significant. Nevertheless, with more monitors in a dispersive region like the LBE line, increased flexibility could be achieved with respect to measurements of additional beam parameters like dispersion and momentum spread.

In the Linac4 dump line the obtained emittance at monitor 1 will have to be corrected for the emittance growth from the Linac4 exit to the first monitor to yield the emittance at the end of Linac4.

Otherwise it has been shown that the method and proposed setups are very robust to systematic errors. Error studies with respect to monitor alignment and quadrupole settings, and errors in the knowledge of the transfer matrix elements between the beam monitors have been considered. They have been judged to be acceptable at the level of a few percent.

Nevertheless, the method turns out to result in not acceptable errors in the Linac4 dump line during the Linac4 commissioning phase, if the input beam parameters and therefore the transfer matrices would deviate too much from the expected values. During this period it is proposed to use an iterative method, which still has to be studied, but should in principle work with the same hardware.

As a summary, the following extensions/modifications of the two lines need to be implemented.

- **Linac4 Dump Line**

Three retractable screens with cameras have to be installed at the specified locations, and a quadrupole has to be added after the horizontal bending magnet. An additional transformer will allow to measure the fraction of beam sent to the dump and could be used to automatically choose transfer matrices corresponding to the beam current in use if wished. At last, the current preliminary dump design will have to be adapted.

- **LBE line**

Three retractable screens with cameras have to be installed at the specified locations. The two existing



quadrupoles need to be exchanged and the first steerer magnet slightly displaced downstream. A dump will be required at the end of the line to allow the use of the line for the Linac4 H<sup>-</sup>-beam in parallel to the ion beam characterisation. One of the existing transformers needs to be exchanged.

With this method and assuming measurement devices with sufficient spatial resolution, it should be possible to measure the transverse emittances of the Linac4 beam in the two lines with an error smaller than the required 10% at the position of the first monitor after the Linac4 commissioning phase.

## Acknowledgements

We are very grateful for initial discussions with R. Scrivens concerning the Three-Monitor-Method. We would like to acknowledge the collaboration with the Linac4 beam dynamics team, to name A. Lombardi, G. Bellodi, M. Eshraqi, S. Lanzone and J-B. Lallement, who provided the initial beam distributions and valuable feedback. We also appreciated the fruitful information exchange with the beam instrumentation group and in particular with E. Bravin, B. Cheymol and F. Roncarolo. Many thanks to A. Lombardi and C. Carli for their constructive comments to this publication.

**A Configuration File for the Linac4 Dump Line in TRACE 3-D**

&amp;DATA

```

ER = 939.29431  Q = -1.0000  W = 158.91167  XI = 65.000
EMITI = 2.848559      2.710997      888.7441
BEAMI = -3.397184     10.02358      0.971066      2.714232     -0.131472     0.028055
BEAMF = 0.00000      0.00000      0.00000      0.00000      0.00000      0.00000
BEAMCI = 0.00000     0.00000      0.00000      0.00000      0.00000      0.00000

```

```

FREQ = 352.200  PQEXT = 2.50  ICHROM = 0  IBS = 0  XC = 0.0000

```

```

XM = 25.0000  XPM = 5.0000  YM = 40.00  DPM = 30.00  DWM = 500.00  DPP = 10.00

```

```

DISPR = 0.000  BETAX = 0.000  BETAY = 0.000
XMI = 10.000  XPMI = 10.000  XMF = 15.000  XPMF = 15.000
DPMI = 30.000  DPMF = 30.000  DWMI = 500.000  DWMF = 500.000

```

```

N1 = 1  N2 = 26  NEL1 = 1  NEL2 = 24  NP1 = 1  NP2 = 26  SMAX = 5.0  PQSMAX = 2.0

```

```

CMT(001)=' 119 Drift01      '  NT(001)= 1  A(1,001)= 118.83700
CMT(002)=' 219 Quad1001    '  NT(002)= 3  A(1,002)= 1.00000 100.0 0.0 0.0 0.0
CMT(003)=' 337 Steerer1    '  NT(003)= 1  A(1,003)= 118.30500
CMT(004)=' 1337 Steerer2   '  NT(004)= 1  A(1,004)= 1000.00000
CMT(005)=' 1487 PU1        '  NT(005)= 1  A(1,005)= 150.00000

CMT(006)=' 2994 Drift      '  NT(006)= 1  A(1,006)= 1507.00000

CMT(007)=' 3144 PU2        '  NT(007)= 1  A(1,007)= 150.00000
CMT(008)=' 3496 Edge       '  NT(008)= 1  A(1,008)= 352.22000
CMT(009)=' 4496 Bending    '  NT(009)= 1  A(1,009)= 1000.00000
CMT(010)=' 4848 Edge       '  NT(010)= 1  A(1,010)= 352.22000

CMT(011)=' 5048 Drift      '  NT(011)= 1  A(1,011)= 200.00000
CMT(012)=' 5390 Quad1001   '  NT(012)= 3  A(1,012)= -2.50000 342.0 0.0 0.0 0.0
CMT(013)=' 5540 Drift      '  NT(013)= 1  A(1,013)= 150.00000

CMT(014)=' 5790 Mon1Front  '  NT(014)= 1  A(1,014)= 250.00000
CMT(015)=' 6040 Mon1Back   '  NT(015)= 1  A(1,015)= 250.00000

CMT(016)=' 8140 Drift      '  NT(016)= 1  A(1,016)= 2100.00000

CMT(017)=' 8390 Mon2Front  '  NT(017)= 1  A(1,017)= 250.00000
CMT(018)=' 8640 Mon2Back   '  NT(018)= 1  A(1,018)= 250.00000

CMT(019)=' 9300 Drift      '  NT(019)= 1  A(1,019)= 660.00000

CMT(020)=' 9550 Mon3Front  '  NT(020)= 1  A(1,020)= 250.00000
CMT(021)=' 9800 Mon3Back   '  NT(021)= 1  A(1,021)= 250.00000

CMT(022)=' 10300 Drift     '  NT(022)= 1  A(1,022)= 500.00000

CMT(023)=' 11800 Dump Conc1 '  NT(023)= 1  A(1,023)= 1500.00000
CMT(024)=' 11900 Dump Air   '  NT(024)= 1  A(1,024)= 100.00000
CMT(025)=' 12400 Dump Core  '  NT(025)= 1  A(1,025)= 500.00000
CMT(026)=' 13900 Dump Conc2 '  NT(026)= 1  A(1,026)= 1500.00000

```

&amp;END

**B Configuration File for the LBE Line in TRACE 3-D**

&amp;data

```

CERN
CH - 1211 Geneva 23
Switzerland

```

```

Geneva, November 23, 2009

```

```

ER = 939.294, Q=-1.0, W=159.16842153283, XI=65.00
EMITI = 3.284, 3.745, 1944.164
BEAMI = -0.211, 5.357, 2.520, 22.978, 15.209, 4.038
BEAMCI = 0.0, 0.0, 0.0, 0.0, 0.0, 0.0
BEAMF = 0.00000, 0.00000, 0.00000, 0.00000, 0.00000, 0.00000

FREQ = 352.210, PQEXT = 2.50, ICHROM = 0.0, IBS = 0, XC = 0.00000

YM = 20.0, DPP = 100
XMI = 10.0, XPMI = 10.0, DPMI = 180.0, DWMI = 500
XMF = 10.0, XPMF = 10.0, DPMF = 180.0, DWMF = 500
DISPR= -2.5

N1 = 1, N2= 29, NEL1 = 1, NEL2 = 21, NP1 = 1, NP2 = 29, SMAX = 5.0, PQSMAX = 2.5, IBS = 0

CMT(001)=' 0 EdgeA ' NT(001)= 9, A(1,001)= 0.0000, 9000.0, 100.0, 0.45, 2.80
CMT(002)=' 900 Dipole ' NT(002)= 8, A(1,002)= 5.7296, 9000.0, 0.0, 0
CMT(003)=' 900 EdgeB ' NT(003)= 9, A(1,003)= 5.7296, 9000.0, 100.0, 0.45, 2.80

CMT(004)=' 6296 Drift ' NT(004)= 1, A(1,004)= 5396

CMT(005)=' 6438 Drift ' NT(005)= 1, A(1,005)= 135
CMT(006)=' 6900 Quad 1 ' NT(006)= 3 A(1,006)= 0.60 462 0.0 0.0 0.0
CMT(007)=' 7042 Drift ' NT(007)= 1, A(1,007)= 149

CMT(008)=' 8190 Drift ' NT(008)= 1, A(1,008)= 1148

CMT(009)=' 8507 Drift ' NT(009)= 1, A(1,009)= 242
CMT(010)=' 8969 Quad 2 ' NT(010)= 3 A(1,010)= -1.90 462 0.0 0.0 0.0
CMT(011)=' 9286 Drift ' NT(011)= 1, A(1,011)= 392

CMT(012)=' 9536 Mon1Front ' NT(012)= 1, A(1,012)= 250
CMT(013)=' 9786 Mon1Back ' NT(013)= 1, A(1,013)= 250

CMT(014)='10081 Steerer ' NT(014)= 1, A(1,014)= 295

CMT(015)='11831 Drift ' NT(015)= 1, A(1,015)= 1750
CMT(016)='12081 Mon2Front ' NT(016)= 1, A(1,016)= 250
CMT(017)='12331 Mon2Back ' NT(017)= 1, A(1,017)= 250
CMT(018)='12732 Drift ' NT(018)= 1, A(1,018)= 401

CMT(019)='13179 Trafo ' NT(019)= 1, A(1,019)= 447

CMT(020)='13279 Drift ' NT(020)= 1, A(1,020)= 100
CMT(021)='13529 Mon3Front ' NT(021)= 1, A(1,021)= 250
CMT(022)='13779 Mon3Back ' NT(022)= 1, A(1,022)= 250
CMT(023)='14411 Drift ' NT(023)= 1, A(1,023)= 632

CMT(024)='14711 SEMGrid ' NT(024)= 1, A(1,024)= 300

CMT(025)='15211 Drift ' NT(025)= 1, A(1,025)= 500
CMT(026)='16711 Dump Conc1 ' NT(026)= 1, A(1,026)= 1500
CMT(027)='16811 Dump Air ' NT(027)= 1, A(1,027)= 100
CMT(028)='17311 Dump Core ' NT(028)= 1, A(1,028)= 500
CMT(029)='18811 Dump Conc2 ' NT(029)= 1, A(1,029)= 1500
&end

```

## C Further Results for the LBE Line

In Table 19 the results for reconstructed  $\alpha$ ,  $\beta$ , and  $\varepsilon$  for all ten combinations of three monitors in the five monitor measure- Tab. 19 ments are presented.

Monitors	horizontal				vertical			
	$\Delta\alpha_{rel}$	$\Delta\beta_{rel}$	$\Delta J$	$\Delta\varepsilon_{rel}$	$\Delta\alpha_{rel}$	$\Delta\beta_{rel}$	$\Delta J$	$\Delta\varepsilon_{rel}$
1 - 2 - 3	-0.19%	-0.22%	-0.001%	-0.17%	+0.43%	+0.39%	-0.002%	-1.60%
1 - 2 - 4	-1.68%	-1.76%	-0.036%	+1.39%	+0.02%	-0.19%	-0.002%	-1.04%
1 - 2 - 5	-3.39%	-3.53%	-0.142%	+3.25%	-0.43%	-0.89%	-0.015%	-0.40%
1 - 3 - 4	-0.18%	-0.44%	-0.045%	+0.05%	+0.69%	-0.09%	-0.032%	-1.14%
1 - 3 - 5	-0.26%	-0.55%	-0.051%	+0.16%	+0.70%	-0.16%	-0.039%	-1.07%
1 - 4 - 5	+1.22%	+0.86%	-0.087%	-1.25%	+1.20%	+0.13%	-0.059%	-1.36%
2 - 3 - 4	+0.46%	+0.23%	-0.035%	+0.27%	+2.26%	+1.29%	-0.064%	+0.14%
2 - 3 - 5	+0.50%	+0.32%	-0.023%	+0.01%	+1.93%	+1.18%	-0.043%	-0.26%
2 - 4 - 5	+0.43%	+0.24%	-0.022%	+0.08%	+1.86%	+1.12%	-0.041%	-0.27%
3 - 4 - 5	+0.15%	+0.02%	-0.010%	+0.56%	+2.05%	+1.41%	-0.041%	+0.05%

**Table 19:** Deviation of reconstructed beam parameters of the three monitor subsets in the five monitor sample (referred to the reference values at beam monitor 1).

## List of Figures

1	Analysis Flow . . . . .	4
2	Dump Line: Phase Space at Linac4 Exit . . . . .	5
3	Layout Dump Line . . . . .	5
4	Dump Line: Reference Phase Space Distributions at monitor 1 (65 mA) . . . . .	7
5	Dump Line: Emittance and Beam Size Evolution (horizontal, 65 mA) . . . . .	7
6	Dump Line: Emittance and Beam Size Evolution (vertical, 65 mA) . . . . .	8
7	Dump Line: Emittance Deviation versus Monitor Resolution . . . . .	8
8	Dump Line: Fitted Beam Size Histograms . . . . .	9
9	Layout LBE Line . . . . .	12
10	LBE Line: Emittance Evolution . . . . .	14
11	LBE Line: Beam Size Evolution . . . . .	14
12	LBE Line: Emittance Deviation versus Monitor Resolution . . . . .	15
13	LBE Line: Reference Phase Space Distributions . . . . .	16
14	LBE Line: Fitted Beam Size Histograms . . . . .	16
15	LBE Line: Iterative Reconstruction of Emittance Values . . . . .	17

## List of Tables

1	Dump Line Parameters (Beam Input and Quadrupole Settings) . . . . .	6
2	Dump Line: Positions of Beam Monitors . . . . .	6
3	Dump Line: Transfer matrix elements between monitors (65 mA) . . . . .	6
4	Dump Line: Beam Sizes (65 mA) . . . . .	8
5	Dump Line: Deviations of Reconstructed Ellipse Parameters (65 mA) . . . . .	10
6	Dump Line: Beam Sizes for 20 and 40 mA . . . . .	10
7	Dump Line: Reconstructed Beam Parameters (20 and 40 mA) . . . . .	10
8	Dump Line: Beam Size versus Transfer Matrix for 20, 40 and 65 mA . . . . .	11
9	Dump Line: Transfer matrix coefficients and emittance deviations for half the longitudinal emittance (65 mA) . . . . .	11
10	LBE Line Parameters (Beam Input and Quadrupole Settings) . . . . .	13
11	LBE Line: Positions of Beam Monitors . . . . .	13
12	LBE Line: Transfer Matrix Elements . . . . .	13
13	LBE Line: Beam Sizes . . . . .	15
14	LBE Line: Ellipse Reconstruction Results (Three Monitors) . . . . .	16
15	LBE Line: Ellipse Reconstruction Results for Modified $\varepsilon_L$ (Three Monitors) . . . . .	18
16	LBE Line: Ellipse Reconstruction Results for Modified $\varepsilon_L$ and Twiss Parameters (Three Monitors) . . . . .	19
17	LBE Line: Positions of Beam Monitors (Five Monitors) . . . . .	19
18	LBE Line: Ellipse Reconstruction Results (Five Monitors) . . . . .	20
19	LBE Line: Three Monitor Results for Five Monitor Measurements . . . . .	25

## References

- [1] H. Wiedemann. *Particle Accelerator Physics*. Springer-Verlag, 2007.
- [2] K. R. Crandall and D. P. Rusthoi. *TRACE 3-D Documentation*, May 1997.
- [3] A. Perrin, J.-F. Amand, T. Muetze, and J.-B. Lallement. *Travel User Manual 4.07*, April 2007.
- [4] G. Cowan. *Statistical Data Analysis*. Oxford University Press Inc., New York, 1998.
- [5] F. Roncarlo et al. *Notes on Scintillating Screens for Linac4-PSB H-Transfer at 160 MeV*, 2009. To be published.
- [6] B. Cheymol. *Private Communication; based on simulations*, 2009.
- [7] A. Lombardi. *Private Communication*, 2009.
- [8] C. Oliver, P.A.P. Nghiem, and C. Marolles. *Transverse Emittance and Energy Spread Measurements for IFMIF-EVEDA*, 2008. Proceedings of Workshop on "Transverse and Longitudinal Emittance Measurement in Hadron-(Pre)Accelerators", Available on → [adweb.desy.de/mdi/CARE/Bad\\_Kreuznach/ABI\\_workshop\\_2008.html](http://adweb.desy.de/mdi/CARE/Bad_Kreuznach/ABI_workshop_2008.html) .
- [9] P. Tetù. *Mesure Impulsion à Impulsion des Trois Plans de Phase du Faisceau du Linac à 50 MeV*. Technical report, CERN PS/LR/Note 79 - 4, 1979.
- [10] CERN Technical Drawings. *Layout Machine Ligne LTB (Sector 2) and references therein*. Available on → <https://edms.cern.ch>, Document PS LMLTB 8003.
- [11] CERN Technical Drawings. *Ligne LTB (LBE Line) and references therein*. Available on → <https://edms.cern.ch>, Document PS LMLTB 8005.